Allosteric Modulator of Mas-Related G-Protein Coupled Receptor X1 (MrgprX1) Inhibits Persistent Pain

by
Zhe Li

A thesis submitted to Johns Hopkins University in conformity with the requirements for the degree of Doctor of Philosophy

Baltimore, Maryland

January, 2016

ABSTRACT

Mas-related G-protein-coupled receptor subtype C and subtype X1 (mouse MrgprC11, rat MrgprC and human MrgprX1) are a novel group of receptors as promising targets of pain inhibitors, mainly because of their restricted expression in small diameter nociceptors within the peripheral nervous system. Drug screens have been conducted targeting at human MrgprX1. However, constrained by the species difference across Mrgprs, many drug candidates could activate MrgprX1 but not the rodent ones, leaving no animal model responsive to test the anti-chronic pain effect *in vivo*. Our laboratory recently generated a transgenic mouse line in which we replaced a cluster of twelve mouse Mrgprs (including MrgprC11) with human MrgprX1. This valuable humanized mouse line allowed us to characterize a potent positive allosteric modulator of MrgprX1, ML382. Cellular studies in humanized MrgprX1 mice suggest that ML382 enhances the ability of bovine adrenal medulla peptide (BAM22, or BAM8–22) as the orthosteric agonist to inhibit N-type voltage-activated calcium current through pertussis toxin sensitive $G_{i/o}$ pathway. We then used several behavior tests to evaluate the analgesic effect of ML382 in inflammatory pain and neuropathic pain animal models. We also observed that MrgprX1 expressing animals developed strong conditioned place preference to ML382 paired chamber comparing to saline paired chamber. Importantly, ML382 effectively attenuates evoked persistent and spontaneous pain without causing peripheral or central side effects such as itch, motor dysfunction, or being rewarding for the uninjured naïve animals. Our findings suggest that humanized MrgprX1 mice provide an essential preclinical model and that allosterically activating MrgprX1 by ML382 is a novel and effective way of inhibiting persistent pain.

Ph.D. DISSERTATION REFEREES FOR ZHE LI

Xinzhong Dong, Ph.D. Professor, Department of Neuroscience (faculty sponsor)

Solomon H. Snyder, M.D. Professor, Department of Neuroscience (reader)

ACKNOWLEDGEMENTS

I would like to thank my advisor, Dr. Xinzhong Dong for his guidance and encouragement during my five years in his laboratory. I am very grateful of him for giving me a much deeper appreciation for science. He is a sharp yet kind hearted mentor and friend. He walked me through my bad days and good days. I will not forget the day when we sat in my electrophysiology room and I almost abandoned the transgenic mouse line of Mrgprx1 because I was not able to detect the expression of this protein. He asked me to give a final shoot by mating it into *Mrgpr-clusterΔ*$^{-/-}$ and detecting the receptor activity directly. This mouse line finally revealed itself as a nice thesis project that kept me busy for several years. I also benefit a lot from Xinzhong's broad collaboration including scientists and physicians. Exposing to collaborative projects and seminars sparked my interest in the pain and itch field from bench top to bed side.

I would like to also express my appreciation for my thesis committee and the faculty who have offered much invaluable advice about thesis projects, troubleshooting and career choices. Dr. Paul Fuchs has spent many afternoons in my recording room to share his expertise of electrophysiology with me. I also appreciate his love for family, science and music. Dr. Mike Caterina has guided me throughout the struggles in my research. He always knows the answer to everything. Dr. Solomon Snyder has been my role model for his enthusiasm to science and education and his wisdom about life. I also want to thank Dr. Carolyn Machamer, the director of BCMB PhD program, for bringing me into Hopkins at the first place and for helping me continuously throughout my career here as a graduate student. She is always there to calm me down and cheer me up when things happen.

I also want to recognize my close collaborators in the lab, Qin Liu (ex-postdoc), Liang Han (ex-postdoc), Yixun Geng, Shuohao Sun, Qin Zheng, Qian Xu, Colleen LaVinka, Kyoungsook Park (ex-postdoc), Hao-Jui Weng (ex-grad) etc. for their friendship, opinions and contributions. They have made my time in the lab memorable and fun. They have also witnessed the two most precious moments in my life when I got married and when I became a mom and

blessed me genuinely. I literally have spent the best five years in my life here, especially during the time when my husband Pang-Yen Tseng joined our lab (I really appreciate Xinzhong for his support of family). I learned so much about electrophysiology and data analysis from my husband. He also taught me to appreciate who I am and embrace my true self before starting chasing goals after goals. With him there are no impossibilities and any success without him would be meaningless.

I will always be indebted to my parents for their immense love and support from thousands of miles away. I want to thank them for those long calls when I needed encouragement to carry on and for putting aside their own career to take care of me and my son. I also want to dedicate this work to my son, Johann Tseng. A whole new world opened up to me from the moment he was born, just like a beam of sunlight from the Infinite and Eternal. I am looking forward to years and years of learning whatever he wants to teach me.

TABLE OF CONTENTS

List of Tables

LIST OF FIGURES

CHAPTER 1: INTRODUCTION

Persistent pain is a major health care problem and yet it is hard to manage partly because it requires sustained application of pain relief over the duration of the chronic pain. However, repetitive application of many pain treatments (e.g. systemic opioids) often decreases the analgesic response and the long term impact of undesired side effects (e.g. sedation, nausea, constipation, addiction, etc.) can further deteriorate life quality in addition to chronic pain itself (Portenoy, 1996; Breivik et al., 2006).

One reason that most pain medicines produce an extensive array of side effects is the broad expression of drug targets (e.g. opioid receptors, cyclooxygenase-2 or COX-2, calcium channels, etc.) in the central and peripheral nervous system, immune pathways, cardiovascular system, etc. (Scholz and Woolf, 2002). Hence, a more pain-selective pharmacologic intervention should target at receptors that express exclusively inside the pain pathway. Especially, chronic pain is often primed with peripheral pathological conditions such as inflammation and nerve injury that sensitize nociceptors (Basbaum et al., 2009; Pope et al., 2013). It would be of great value to identify novel molecular targets on nociceptive sensory neurons in the trigeminal and dorsal root ganglia (DRG) (He et al., 2014).

G protein-coupled receptors (GPCRs) have been very fruitful drug targets in recent years. One potential target is the Mas-related G-protein–coupled receptor (Mrgpr), which is a family of orphan GPCRs consisting of many genes in human, rat and mouse (Dong et al., 2001; Lembo et al., 2002; Choi and Lahn, 2003; Zhang et al., 2005; Gloriam et al., 2007). Many *Mrgpr*s, such as mouse *MrgprA3*, *MrgprC11, MrgprD,* rat *MrgprC* and human *MrgprX*s, are expressed specifically in small-diameter afferent neurons (presumably nociceptive) and have been reported to play important roles in peripheral sensation (Zylka et al., 2003; Conn et al., 2009; Liu et al., 2009; Guan et al., 2010; Sikand et al., 2011; Liu et al., 2012; Han et al., 2013; He et al., 2014; He et al., 2014). For example, subcutaneous chloroquine induces strong scratching behavior in mice

through MrgprA3 (Liu et al., 2009). Activation of MrgprC with agonists such as bovine adrenal medulla peptide (BAM) 8–22 and JHU58 (by intrathecal [i.th.] application) attenuates persistent pain in an MrgprC-dependent manner in rodents (Guan et al., 2010; He et al., 2014).

Interestingly, *Mrgpr-clusterΔ*$^{-/-}$ mice (which have a deletion of 12 Mrgprs, including MrgprA3 and MrgprC11) display enhanced spontaneous pain responses in the inflammatory phase of formalin-induced pain (Guan et al., 2010). They also have a prolonged phase of mechanical hypersensitivity in the L5 sciatic chronic constriction injury model (He et al., 2014). Therefore, we have been interested to investigate the analgesic effect of human MrgprX1 under chronic pain condition for potential clinical application. However, constrained by the species difference across Mrgprs, many drug candidates activate MrgprX1 but not the rodent ones. The progress of further developing these drugs is impeded due to the lack of animal model to test the anti-chronic pain effect *in vivo*. In this article, we report the generation of a transgenic mouse line in which *MrgprX1* gene is expressed in *Mrgpr*-expressing primary sensory DRG neurons.

Rodent MrgprCs and MrgprX1 has been reported for both analgesic and pruritogenic effect (Liu et al., 2009; Guan et al., 2010; Sikand et al., 2011; Han et al., 2013; Jiang et al., 2013; He et al., 2014). To avoid inducing itch by the activation of peripherally expressed MrgprX1, we used the strategy of allosterically enhancing the endogenous activity of MrgprX1 at the site where receptor and endogenous ligand co-exist, i.e., at the central terminal (See model in Fig. 1.1). Mrgpr^{+} DRG neurons terminate both centrally at spinal cord lamina II and peripherally at skin (Han et al., 2013). BAM22 immunoreactivity was found in several tissues including brain and superficial spinal cord dorsal horn (Mizuno et al., 1980; Hollt et al., 1982; Cai et al., 2007; Solinski et al., 2014). Therefore, we perform our behavioral study by intrathecal application of allosteric modulator candidates to investigate analgesic effect exclusively.

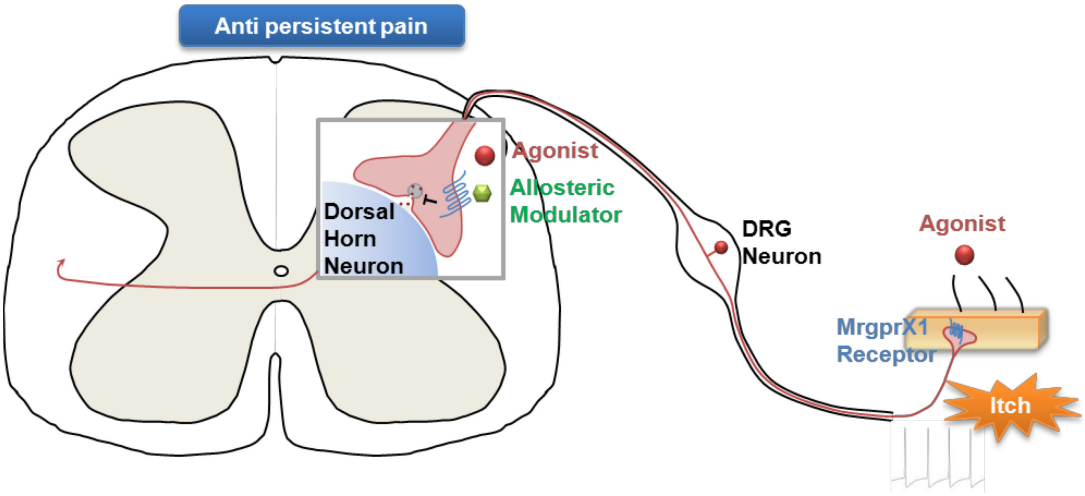

Figure 1.1 The central and peripheral function of MrgprX1$^+$ DRG neurons. A model showing the functional compartmentation of MrgprX1$^+$ DRG neurons. Peripheral activation of MrgprX1 receptor with exogenous agonist produces action potential and generates itch sensation. In persistent pain condition, central activation of MrgprX1 inhibits synaptic input into spinal cord dorsal horn neurons to attenuate persistent pain. BAM peptide is an endogenous agonist of MrgprX1. Exogenous allosteric modulator can enhance the activation of MrgprX1 by endogenous agonist.

Allosteric modulators have become a popular direction in the drug discovery for GPCRs. It binds to the allosteric site and modulates the responsiveness of its receptor together with the binding of orthosteric ligand (Conn et al., 2009). It can offer high selectivity since the orthosteric binding sites are often conserved across a GPCR subfamily. It also allows a better temporal and spatial control of modulating endogenous physiological signaling due to the requirement of endogenous orthosteric ligand binding. Further, screening for allosteric modulators in the pool of small molecule compounds provides the possibility of better penetration of blood brain barrier and therefore multiple drug delivery methods other than intrathecal (Wen et al., 2015).

In this study, we performed screening for allosteric modulators of MrgprX1 and got a candidate ML382. We also demonstrate that activation of MrgprX1 by BAM8–22 reduces neurotransmitter release by inhibiting N-type voltage-activated calcium current through PTX sensitive $G_{i/o}$ pathway. MrgprX1 agonist BAM22 (endogenous) is up-regulated at spinal cord dorsal horn under chronic pain condition. We hypothesize that positive allosteric modulator ML382 could enhance the potency of BAM22 at MrgprX1 to attenuate persistent pain.

CHAPTER 2: ML382 IS A CANDIDATE OF ALLOSTERIC MODULATOR OF MRGPRX1

Introduction

GPCRs represent the largest class of cell-surface receptors and have been implicated in numerous disorders (George et al., 2002). Despite almost half of all modern drugs regulate the activity of GPCR activity in some way, the majority of GPCRs have not successfully been targets by useful ligands yet (Conn et al., 2009). It is often difficult to develop ligands with high selectivity at specific GPCR subtypes because their orthosteric binding sites can be highly conserved across a GPCR subfamily; plus it is often infeasible to develop small molecule drugs for some GPCRs whose orthosteric binding sites are designed for peptides or proteins (Conn et al., 2009). Researchers therefore tried to approach with selective allosteric modulators, which bind to allosteric binding sites and either potentiate or inhibit the activation of the receptors by their endogenous orthosteric ligands (May et al., 2007).

Developing drugs targeting at MrgprX1 has an extra fold of conundrum, that directly activating MrgprX1 at peripheral terminals induces itch in rodents and humans (Liu et al., 2009; Sikand et al., 2011). Therefore, targeting this receptor with an orthosteric activating drug is an unviable approach to pain relief. Allosteric ligands that bind at allosteric binding sites provide better specificity than orthosteric ligands alone because they require co-localization of receptor and orthosteric ligand to function. As long as the endogenous orthosteric ligand of MrgprX1 is restricted at the pain-processing central terminal of DRG neurons, the allosteric drug would function only there even when it is administrated systemically.

We therefore conducted a screen of the 307000 NIH Molecular Library Small Molecule Repository (MLSMR) compound collection using a triple addition protocol with BAM8–22 as the orthosteric ligand (Assay ID: 588675) with the help of Vanderbilt Center for Neuroscience Drug Discovery. The flow chart of screening paradigm for positive allosteric modulator of MrgprX1 is as listed in Fig. 2.1.

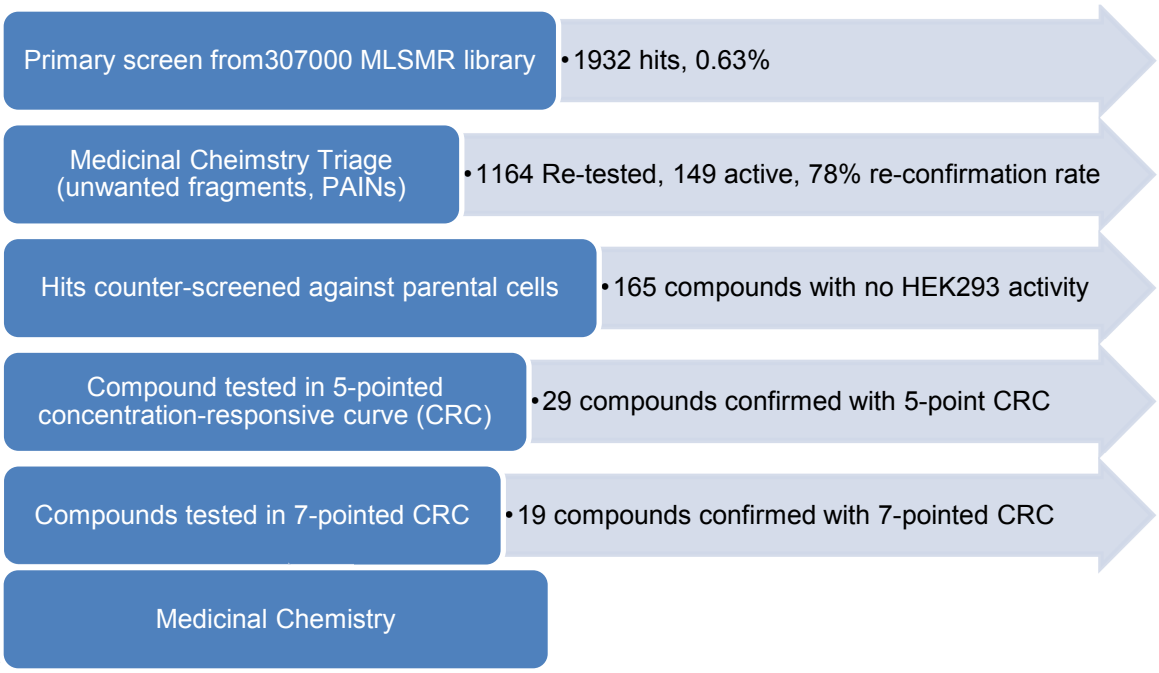

Figure 2.1 Flowchart of the screening paradigm for allosteric modulators of MrgprX1 (adapted from Wen et al.) (2015).

Methods

Screen using FLIPR Calcium Imaging

HEK293 wild type cells or HEK293 cells stably expressing MrgprX1 were cultured on poly-D-lysine coated 96-well plate overnight. Center point confluency should be around 90%–100% at the time of the assays. FLIPR Calcium Assay 5 kit (Molecular Devices, Sunnyvale, CA) was used as free calcium ratiometric indicator. After incubating with the indicator solution for 40 min at 37°C followed by 10 min at room temperature, the plate was loaded in the Flexstation machine. Each well contained 100μL solution initially and was then incubated with 50μL candidates of positive allosteric modulators (diluted in 1×HBSS + 20mM HEPES) or vehicle for 80 sec. Then 50μL BAM8–22 (10nM, very low dose) or vehicle was added. Compound plates of BAM8–22 were coated with 1% BSA (to avoid BAM8–22 sticking to the wall of the plate for 1hr prior to FLIPR assays. Tips were changed between each cell plate and each drug plate. Readings were compared between the candidates and vehicle to see whether the candidates could increase BAM8–22 response. [Reading = (candidate-BAM−vehicle-BAM) ÷ (vehicle-BAM−vehicle-vehicle) ×100%]. The reading of each candidate was replicated in three wells and the promising candidates were repeated later again for dose response curve.

Liquid Chromatography/Mass Spectrometry Analysis (LC/MS/MS) of ML382 in the Cerebral Spinal Fluid

ML382 was analyzed via electrospray ionization (ESI) on an AB Sciex API-4000 (Foster City, CA) triple-quadrupole instrument that was coupled with Shimadzu LC-10AD pumps (Columbia, MD) and a Leap Technologies CTC PAL auto-sampler (Carrboro, NC). Analytes were separated by gradient elution using a Fortis C18 2.1 x 50 mm, 3.5 μm column (Fortis Technologies Ltd, Cheshire, UK) thermostated at 40 °C. HPLC mobile phase A was 0.1% NH_4OH (pH unadjusted), mobile phase B was acetonitrile. The gradient started at 30% B after a 0.2 min

hold and was linearly increased to 90% B over 0.8 min; held at 90% B for 0.5 min and returned to 30% B in 0.1 min followed by a re-equilibration (0.9 min). The total run time was 2.5 min and the HPLC flow rate was 0.5 mL/min. The source temperature was set at 500°C and mass spectral analyses were performed using multiple reaction monitoring (MRM) utilizing a Turbo-Ionspray® source in positive ionization mode (5.0 kV spray voltage). LC/MS/MS analysis was performed employing a TSQ Quantum^{ULTRA} that was coupled to a ThermoSurveyor LC system (Thermoelectron Corp., San Jose, CA) and a Leap Technologies CTC PAL auto-sampler (Carrboro, NC). Chromatographic separation of analytes was achieved with an Acquity BEH C18 2.1 x 50 mm, 1.7 µm column (Waters, Taunton, MA).

Plasma Protein Binding

Protein binding of ML382 was determined in human, rat and mouse plasma via equilibrium dialysis employing Single-Use RED Plates with inserts (ThermoFisher Scientific, Rochester, NY). Briefly plasma (220 µL) was added to the 96 well plate containing test article (5 µL) and mixed thoroughly. Subsequently, 200 µL of the plasma-test article mixture was transferred to the cis chamber (red) of the RED plate, with an accompanying 350 µL of phosphate buffer (25 mM, pH 7.4) in the trans chamber. The RED plate was sealed and incubated 4 h at 37 °C with shaking. At completion, 50 µL aliquots from each chamber were diluted 1:1 (50 µL) with either plasma (cis) or buffer (trans) and transferred to a new 96 well plate, at which time ice-cold acetonitrile (2 volumes) was added to extract the matrices. The plate was centrifuged (3000 rpm, 10 min) and supernatants transferred to a new 96 well plate. The sealed plate was stored at -20 °C until LC/MS/MS analysis.

Statistics

Data are presented as mean ± s.e.m. The number of mice analyzed is represented as *n*. Statistical comparisons were conducted by two-tailed, unpaired or paired Student's *t* test

according to experimental design. Statistical significant difference was assumed at $P < 0.05$. Experiments were replicated biologically at least three times.

Results

Calcium mobilization screen suggested ML382 modulates MrgprX1

From the 29 identified "hits" mentioned in Fig. 2.1, there were four compounds from a sulfonamide benzamide series. Combining the activity in the calcium mobilization functional assay and excellent selectivity profile as observed in the PubChem Assay and PubChem Hit rate (Assay ID: 588675), this series was chosen for further modification toward a novel positive allosteric modulator of MrgprX1. Then 19 modified compounds went through further screening (Assay ID: 743016), yielding ML382 of the highest potency and efficacy (Wen et al., 2015).

The dose-response studies show that 5 μM ML382 enhances the potency of BAM8–22 on MrgprX1 by >7-fold (i.e., EC50 of BAM8–22 from 18.7 to 2.9 nM; Fig. 2.2A). However, ML382 does not affect the Emax of BAM8–22 if the maximum concentration of BAM8–22 is used (Fig. 2.2A). Furthermore, ML382 does not activate MrgprX1 in the absence of BAM8–22, suggesting ML382 itself does not has agonistic activity toward MrgprX1 (Fig. 2.2B). Pharmacological and selectivity profiling of ML382 were performed against the closely related MrgprX2 in HEK293 stable cell line expressing MrgprX2 as a selectivity screen. The orthosteric agonist we used was proadrenomedullin amino-terminal 20 peptide, fragment 9-20 (PAMP(9-20)) (Kamohara et al., 2005). ML382 showed no significant effect on the activation of MrgprX2 in the presence of the specific agonist peptide, PAMP (neither EC50 nor Emax) (Fig. 2.2C).

A

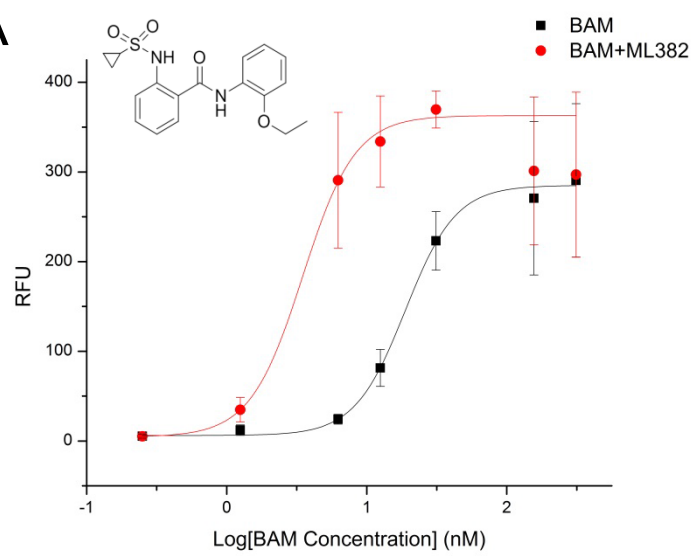
BAM
BAM+ML382
RFU
Log[BAM Concentration] (nM)

B

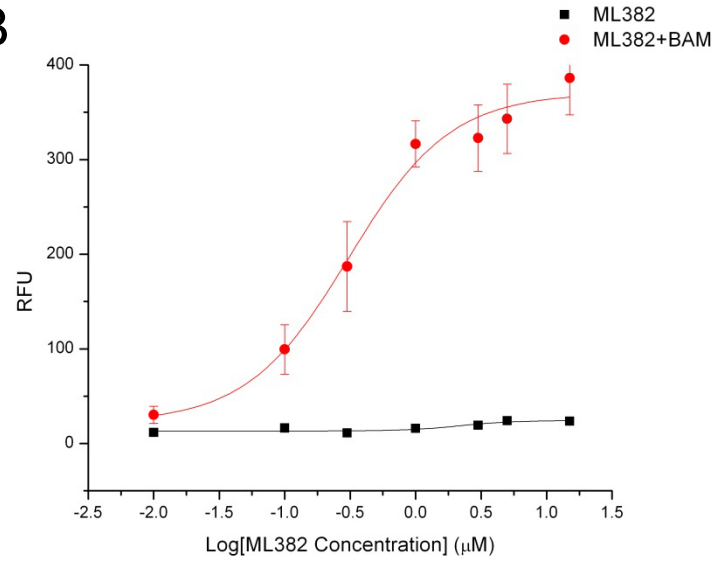
ML382
ML382+BAM
RFU
Log[ML382 Concentration] (μM)

C

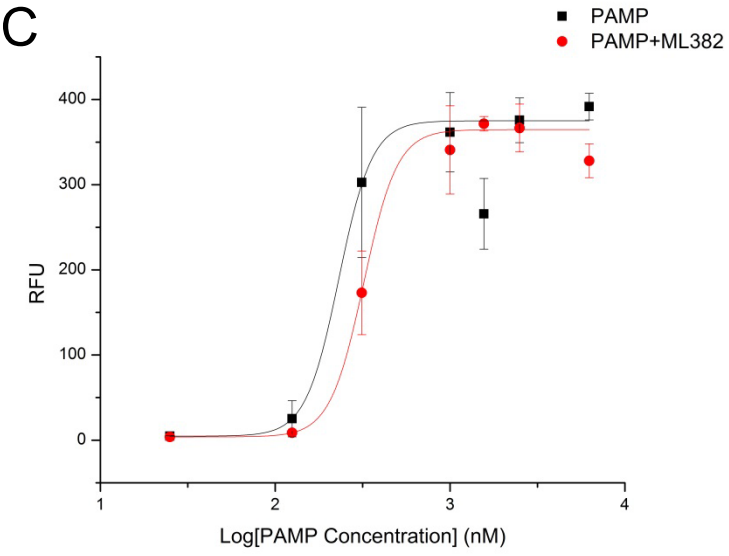
PAMP
PAMP+ML382
RFU
Log[PAMP Concentration] (nM)

Figure 2.2 Pharmacological profile of ML382 on MrgprX1-expressing HEK293 cells. (A) ML382 enhances the potency of BAM8–22 on MrgprX1-expressing HEK293 cells. Dose-response curve of BAM8–22 in presence (red dots) or absence of ML382 (black squares) was determined by Ca^{2+} mobilization assays. The EC50 of BAM8–22 in presence of maximal amount of ML382 (5 μM) is 2.87 ± 1.22 nM (95% confidence interval). In the absence of ML382 (black squares), the EC50 of BAM8–22 is 18.67 ± 1.06 nM (95% confidence interval). Inset: the chemical structure of ML382. **(B)** Dose-response curve of ML382 in the presence (red dots) and absence (black squares) of BAM8–22 as determined by Ca^{2+} mobilization assays. The EC50 value of ML382 in the presence of submaximal amounts of BAM8–22 (10 nm) is 190 nm. In the absence of BAM8–22 (black squares), ML382 itself does not activate MrgprX1. **(C)** ML382 has no effect on MrgprX2-expressing HEK293 cells. Dose-response curve of PAMP in presence (red circles) or absence of ML382 (black squares) was determined by Ca^{2+} mobilization assay. The EC50 of PAMP in presence of 5 μM ML382 is 316.12 ± 17.8 nM (95% confidence interval). In the absence of ML382, the EC50 of BAM8–22 is 211.86 ± 51.98 nM (95% confidence interval). RFU: relative fluorescence units; values are the mean ± SEM of three repeat experiments, and data points are fitted to a sigmoidal variable slope dose-response curve.

In addition, ML382 was evaluated using the Eurofins Lead Profiling Screen, which is a binding assay panel of 68 GPCRs, ion channels, and transporters screened at 10 μM (Eurofins Scientific: http://www.eurofins.com/en.aspx accessed in August 2014). ML382 did not inhibit 67 of the 68 targets assayed (inhibition of radioligand binding >50% at 10 μM); the only target that was considered active was serotonin (5-hydroxytryptamine) $5HT_{2B}$, which showed 63% inhibition at 10 μM (See materials from Eurofins attached below). Overall, ML382 displayed a very favorable selectivity profile (Wen et al., 2015).

Summary of Significant Results

Biochemical assay results are presented as the percent inhibition of specific binding or activity throughout the report. All other results are expressed in terms of that assay's quantitation method.

- For primary assays, only the lowest concentration with a significant response judged by the assays' criteria, is shown in this summary.
- Where applicable, either the secondary assay results with the lowest dose/concentration meeting the significance criteria or, if inactive, the highest dose/concentration that did not meet the significance criteria is shown.
- Unless otherwise requested, primary screening in duplicate with quantitative data (e.g., IC_{50} ± SEM, K_i ± SEM and n_H) are shown where applicable for individual requested assays. In screening packages, primary screening in duplicate with semi-quantitative data (e.g., estimated IC_{50}, K_i and n_H) are shown where applicable (concentration range of 4 log units); available secondary functional assays are carried out (30 mM) and MEC or MIC determined only if active in primary assays >50% at 1 log unit below initial test concentration.

Significant responses (≥ 50% inhibition or stimulation for Biochemical assays) were noted in the primary assays listed below:

Cat #	Assay Name	Species	Conc.	% Inh.	IC_{50}*	K_I	n_H
271700	Serotonin (5-Hydroxytryptamine) 5-HT$_{2B}$	hum	10 µM	63			

* A standard error of the mean is presented where results are based on multiple, independent determinations.
ham=Hamster; hum=Human

Experimental Results

Cat #	Assay Name	Batch*	Spec.	Rep.	Conc.	% Inh.	IC_{50}*	K_I	n_H	R
Compound: ML382, PT #: 1176873										
200510	Adenosine A_1	344150	hum	2	10 µM	-1				
200610	Adenosine A_{2A}	344151	hum	2	10 µM	-26				1
200720	Adenosine A_3	344148	hum	2	10 µM	10				
203100	Adrenergic α_{1A}	344152	rat	2	10 µM	1				
203200	Adrenergic α_{1B}	344240	rat	2	10 µM	2				
203400	Adrenergic α_{1D}	344154	hum	2	10 µM	6				
203630	Adrenergic α_{2A}	344155	hum	2	10 µM	-13				
204010	Adrenergic β_1	344146	hum	2	10 µM	-3				
204110	Adrenergic β_2	344156	hum	2	10 µM	-11				
206000	Androgen (Testosterone)	344120	hum	2	10 µM	4				
212510	Bradykinin B_1	344119	hum	2	10 µM	28				
212620	Bradykinin B_2	344191	hum	2	10 µM	14				
214510	Calcium Channel L-Type, Benzothiazepine	344415	rat	2	10 µM	-1				
214600	Calcium Channel L-Type, Dihydropyridine	344157	rat	2	10 µM	-6				
216000	Calcium Channel N-Type	344192	rat	2	10 µM	-12				
217030	Cannabinoid CB_1	344158	hum	2	10 µM	-8				
219500	Dopamine D_1	344159	hum	2	10 µM	12				
219700	Dopamine D_{2S}	344160	hum	2	10 µM	-10				
219800	Dopamine D_3	344161	hum	2	10 µM	-18				
219900	Dopamine $D_{4.2}$	344162	hum	2	10 µM	-10				
224010	Endothelin ET_A	344193	hum	2	10 µM	7				
224110	Endothelin ET_B	344122	hum	2	10 µM	-12				
225510	Epidermal Growth Factor (EGF)	344089	hum	2	10 µM	9				
226010	Estrogen ERα	344194	hum	2	10 µM	-3				
226600	$GABA_A$, Flunitrazepam, Central	344164	rat	2	10 µM	11				
226500	$GABA_A$, Muscimol, Central	344163	rat	2	10 µM	0				
228610	$GABA_{B1A}$	344149	hum	2	10 µM	14				
232030	Glucocorticoid	344197	hum	2	10 µM	2				
232700	Glutamate, Kainate	344198	rat	2	10 µM	-1				
232810	Glutamate, NMDA, Agonism	344199	rat	2	10 µM	0				
232910	Glutamate, NMDA, Glycine	344200	rat	2	10 µM	4				
233000	Glutamate, NMDA, Phencyclidine	344165	rat	2	10 µM	5				
239610	Histamine H_1	344166	hum	2	10 µM	-12				
239710	Histamine H_2	344145	hum	2	10 µM	0				

Note: Items meeting criteria for significance (≥50% stimulation or inhibition) are highlighted.
* Batch: Represents compounds tested concurrently in the same assay(s).
ham=Hamster; hum=Human
R=See Remarks (if any) at end of this section.

Experimental Results

Cat #	Assay Name	Batch*	Spec.	Rep.	Conc.	% Inh.	IC_{50}*	K_I	n_H	R
239820	Histamine H_3	344201	hum	2	10 µM	2				
241000	Imidazoline I_2, Central	344181	rat	2	10 µM	-7				
243520	Interleukin IL-1	344202	mouse	2	10 µM	5				
250460	Leukotriene, Cysteinyl $CysLT_1$	344203	hum	2	10 µM	0				
251600	Melatonin MT_1	344138	hum	2	10 µM	7				
252610	Muscarinic M_1	344167	hum	2	10 µM	9				
252710	Muscarinic M_2	344168	hum	2	10 µM	-17				
252810	Muscarinic M_3	344169	hum	2	10 µM	-4				
257010	Neuropeptide Y Y_1	344221	hum	2	10 µM	1				
257110	Neuropeptide Y Y_2	344205	hum	2	10 µM	2				
258590	Nicotinic Acetylcholine	344139	hum	2	10 µM	12				
258700	Nicotinic Acetylcholine α1, Bungarotoxin	344140	hum	2	10 µM	0				
260130	Opiate δ_1 (OP1, DOP)	344206	hum	2	10 µM	0				
260210	Opiate κ(OP2, KOP)	344207	hum	2	10 µM	4				
260410	Opiate µ(OP3, MOP)	344171	hum	2	10 µM	2				
264500	Phorbol Ester	344172	mouse	2	10 µM	0				
265010	Platelet Activating Factor (PAF)	344214	hum	2	10 µM	15				
265600	Potassium Channel [K_{ATP}]	344173	ham	2	10 µM	10				
265900	Potassium Channel hERG	344174	hum	2	10 µM	2				
268420	Prostanoid EP_4	344175	hum	2	10 µM	12				
268700	Purinergic P2X	344208	rabbit	2	10 µM	33				
268810	Purinergic P2Y	344209	rat	2	10 µM	20				
270000	Rolipram	344176	rat	2	10 µM	11				
271110	Serotonin (5-Hydroxytryptamine) 5-HT_{1A}	344211	hum	2	10 µM	-2				
271700	Serotonin (5-Hydroxytryptamine) 5-HT_{2B}	344177	hum	2	10 µM	63				
271910	Serotonin (5-Hydroxytryptamine) 5-HT_3	344210	hum	2	10 µM	8				
278110	Sigma σ_1	344178	hum	2	10 µM	-1				
279510	Sodium Channel, Site 2	344180	rat	2	10 µM	7				
255520	Tachykinin NK_1	344170	hum	2	10 µM	8				
285900	Thyroid Hormone	344215	rat	2	10 µM	1				
220320	Transporter, Dopamine (DAT)	344123	hum	2	10 µM	-5				
226400	Transporter, GABA	344196	rat	2	10 µM	10				
204410	Transporter, Norepinephrine (NET)	344141	hum	2	10 µM	0				
274030	Transporter, Serotonin (5-Hydroxytryptamine) (SERT)	344179	hum	2	10 µM	5				

Note: Items meeting criteria for significance (≥50% stimulation or inhibition) are highlighted.
* Batch: Represents compounds tested concurrently in the same assay(s).
ham=Hamster; hum=Human
R=See Remarks (if any) at end of this section.

In vivo concentration in cerebral spinal fluid and plasma stability of ML382

In order to quantify the concentration of ML382 exposed at spinal cord as a reference for further cellular studies, we dissected the spinal cords out 30 min after intrathecally injecting 10 µL of 250 µM ML382 or 10 µL saline as control and incubated the spinal cord in 500 µL oxygen saturated aCSF (artificial cerebral spinal fluid) at 37°C for an hour. The amount of ML382 in the aCSF was detected using liquid chromatography/mass spectrometry analysis. The amount of ML382 detected is 4.48 ± 2.24 ng/mL (average ± s.e.m., n = 3). Assuming the 10 µL drug is diluted 50 times in the 500 µL aCSF (since the amount of endogenous cerebral spinal fluid is minimal), the concentration is 1.08 ± 0.68 µM. The actual concentration at lumbar region *in vivo* could be higher since the intrathecal injection is between lumbar 5 and sacral 1. The amount of ML382 in the mice which were intrathecally injected with saline was below the limit of quantification. We also measured the level of ML382 over time in plasma and found that it is relatively stable in human and rat plasma but not in mouse plasma (Table 2.1).

Time	Mouse	Rat	Human
0 hr	100%	100%	100%
1 hr	98.47%	102%	103%
4 hr	69.15%	91%	100%

Table 2.1 Pharmacokinetic study of ML382. ML382 was incubated with mouse, rat or human plasma for 0 hr, 1 hr, or 4 hr and then quantified by LC/MC/MC analysis. ML382 was unstable in mouse plasma and stable in rat and human plasma.

Discussion

In summary, we developed ML382 as a potent and selective allosteric modulator of MrgprX1 receptor using calcium mobilization functional assay in HEK293 cells that express this receptor stably. This is the first positive allosteric modulator reported for MrgprX1 (Wen et al., 2015). In the presence of the known ligand BAM8–22, ML382 has an EC50 value of 190 nm with an Emax value of 148% of the effect caused by BAM8–22 alone. It is inactive against the closely related MrgprX2 and against a group of selected receptors from the Eurofins panel. In addition, ML382 was profiled in pharmacokinetic assay and possesses favorable stability in rat and human plasma, which indicates the utility of ML382 as a potential oral dosing regimens (as well as intraperitoneal, subcutaneous, or intrathecal). Further use of ML382 in an *in vivo* animal study and the underlying mechanism is reported in following part of the thesis.

Directly activating MrgprX1 induces itch in rodent and human (Liu et al., 2009; Sikand et al., 2011), making it an intractable drug target using traditional orthosteric ligand approach. ML382 does not activate MrgprX1 receptor directly and thus does not induce scratching behavior. It provided an effective approach to treat chronic pain without inducing itch, which is an advantage over the orthosteric agonist BAM peptide. Allosteric modulation is a well-accepted concept in the field of drug development in recent years, especially for GPCR targets. For example, benzodiazepines are allosteric modulators of γ-aminobutyric acid $(GABA)_A$ receptors without inducing potential lethal effect by directly activating GABA receptor (Mohler et al., 2002; Conn et al., 2009). One of the reasons include that the binding sites across a GPCR subfamily are often highly conserved (Conn et al., 2009). Allosteric ligands that bind at allosteric binding site provide better specificity since they require the co-localization of receptor and orthosteric ligand to function. BAM22 peptide is accumulated at central terminal of sensory neurons during chronic pain condition (see model in Fig. 1.1). Thus ML382 could maximize BAM's effect selectively at spinal cord dorsal horn to attenuate the input from $MrgprX1^+$ nerve terminals to inhibit evoked persistent and spontaneous pain. Besides, orthosteric ligands can be peptides or proteins that

are difficult to pass the brain blood barrier (BBB) when administrated exogenously. Allosteric ligands can be designed and screened in small molecule pools and be modified for better drug metabolism and pharmacokinetics properties. ML382 was screened in small molecule pools and was modified for better potency.

CHAPTER 3: THE MOLECULAR MECHANISM OF MRGPRX1 TO INHIBIT NEUROTRANSMITTER RELEASE INTO SPINAL CORD DORSAL HORN

Introduction

HVA Ca^{2+} channels play an important role in controlling the release of neurotransmitter vesicles from nociceptive DRG neurons into spinal cord neurons (Bao et al., 1998). L-type, P/Q-type, and N-type HVA Ca^{2+} channels have been important targets for the development of drugs to treat pain (McGivern and McDonough, 2004; Gribkoff, 2006; Perret and Luo, 2009). However, because these channels are broadly expressed throughout the peripheral and central nervous systems and the cardiovascular system, channel blockers pose side effects such as nausea, anxiety, and sweating (Staats et al., 2004; Wermeling, 2005; Klotz, 2006). Many GPCRs, including MrgprC11, are known to modulate HVA Ca^{2+} channels (Chen and Ikeda, 2004; Tedford and Zamponi, 2006; Zamponi and Currie, 2013; Li et al., 2014). The most extensively studied examples include μ and κ opioid receptors, which mainly inhibit N-type Ca^{2+} channels and mediate reduction of Ca^{2+}-dependent presynaptic neurotransmitter release to produce an analgesic effect (Macdonald and Werz, 1986; Tsunoo et al., 1986; Moises et al., 1994; Wiley et al., 1997). Since MrgprX1 is more restricted to the pain pathway and can selectively modulate HVA Ca^{2+} channels to attenuate persistent pain, we hypothesized that activating MrgprX1, rather than targeting Ca^{2+} channels directly, can attenuate persistent pain while avoiding most central and peripheral side effects.

The synthetic ligand we used as orthosteric ligand of MrgprX1 was BAM8–22, a truncation of BAM with high potency and specificity to MrgprX1 and rodent MrgprCs (Lembo et al., 2002). The endogenous BAM22 peptide contains the characteristic Met-enkephalin YGGFM motif at the N-terminal that activates classic opioid receptor subtypes (μ, δ, κ) (Mizuno et al., 1980). It is also a potent ligand for MrgprX1 and MrgprC11 (Mizuno et al., 1980; Han et al., 2002; Lembo et al., 2002). Upregulation of BAM22 and MrgprC receptor has been reported in inflammation and nerve injury models (Cai et al., 2007; Jiang et al., 2013; He et al., 2014). BAM8–22 has also been

reported to inhibit HVA I_{Ca} in a previous study using heterologously expressed MrgprX1 in SCG and DRG neurons (Chen and Ikeda, 2004). Therefore Mrgprs may represent an endogenous inhibitory pathway which parallels that of opioid receptors and converges on BAM peptide to neutralize chronic hyperalgesia (Woolf and Salter, 2000; Ji et al., 2003).

Methods

All animal experiments were performed under protocols approved by the Animal Care and Use Committee of the Johns Hopkins University School of Medicine.

Generation of MrgprX1 mice

We purchased a mouse BAC clone (RP23-311C15) containing the entire Mrgpra3 gene from the Children's Hospital Oakland Research Institute. We modified the BAC clone using the homologous recombination in bacteria to generate the *Mrgprc11*^{Mrgprx1} mouse line. We crossed them with *Mrgpra3*$^{GFP\text{-}Cre}$ (Han et al., 2013), and *Mrgpr-clusterΔ*$^{-/-}$ (Liu et al., 2009) lines that was generated in our lab. We used the *Mrgprc11*^{Mrgprx1} transgenic line and *Mrgpra3*$^{GFP\text{-}Cre}$ transgenic line as hemizygotes or heterozygotes for all the experiments.

Primary Cell culture

DRGs from 3–4-week-old mice were collected in cold DH10 medium (DMEM/F-12 with 10% fetal bovine serum and 1% penicillin/streptomycin, Gibco) and treated with enzyme solution (5mg/ml dispase and 1mg/ml collagenase Type I in HBSS without Ca^{2+} and Mg^{2+}, Gibco) at 37°C. After trituration and centrifugation, cells were resuspended in DH10 with nerve growth factor (50ng/ml, Upstate) and glial cell line-derived neurotrophic factor (25ng/ml, R&D Systems), plated on glass coverslips coated with poly-D-lysine (100 μg/ml, Biomedical Technologies) and laminin (10μg/ml, Invitrogen), cultured at 37°C, and used after 20–40 hours (Liu et al., 2009).

Whole-cell recordings of cultured DRG neurons

Whole cell currents of cultured DRG neurons with *Mrgpra3*-GFP marker were recorded with an Axon 700B amplifier and the pCLAMP 9.2 software (Molecular Devices, Sunnyvale, CA, USA). Extracellular solution contains (in mM) 130 N-methyl-D-glucamine chloride (NMDG-Cl), 5 $BaCl_2$, 1 $MgCl_2$, 10 HEPES, and 10 Glucose, with pH of 7.4 adjusted with 1M NMDG. Osmolality was adjusted to 310 mOsm/kg with sucrose. Electrodes were pulled (Model pp-830; Narishige, East Meadow, NY, USA) from borosilicate glass (WPI, Inc., Sarasota, FL, USA) with resistances of 2-4 MΩ. Pipette solution contained 140 Tetraethylammonium chloride (TEA-Cl), 10 EGTA, 1 $MgCl_2$, 10 HEPES, 0.5 GTP, and 3 ATP, with pH of 7.4 and osmolality about 300 mOsm/kg. The voltage protocol was modified from previous paper (Chen and Ikeda, 2004). Briefly, cells were held at -80 mV, evoked to -40 mV for 20 milliseconds (ms) to activate low voltage Ca^{2+} channels, followed by holding to -60 mV for 20 ms, and evoked to -10 mV for 40 ms to activate high voltage activated Ca^{2+} channel. Leak currents were subtracted with P/4 protocol. Liquid junction potentials, whole cell capacitances were offset and series resistances were compensated by 70%. All experiments were performed at room temperature (21–23 °C).

Mechanistic study of allosteric modulation

Dose-dependent curves (Fig. 3.3B) were fitted with Hill equation:

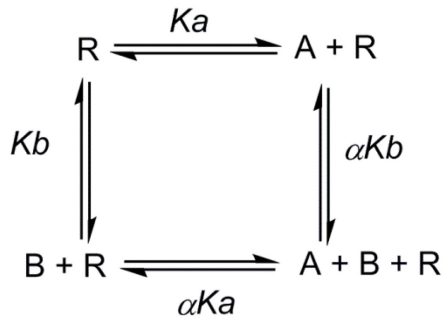

In this scheme, R is the receptor, A is orthosteric ligand, and B is allosteric modulator. Ka and Kb indicate the association constants of ligand O and A, respectively. When both ligands are interacting with the receptor, the two ligands can reciprocally affect the association constants, and the magnitude of this cooperativity is determined by the factor α. The equation which describes the ternary complex model can be derived from above scheme and is shown as following:

(BX51, Melville, NY, USA). Data were acquired with pClamp 10 software (Molecular Devices) and a Multiclamp amplifier. Using a puller (P1000, Sutter, Novato, CA, USA), we fabricated thin-walled glass pipettes (World Precision Instruments, Sarasota, FL, USA) that had a resistance of 3-6 MX and were filled with internal solution (in mM: 120 K-gluconate, 20 KCl, 2 $MgCl_2$, 0.5 EGTA, 2 Na_2-ATP, 0.5 Na_2-GTP, and 20 HEPES). The cells were voltage clamped at –70 mV. Membrane current signals were sampled at 10 kHz and low-pass filtered at 2 kHz. Larger-bore pipettes filled with Krebs solution were used for dorsal root stimulation. To evoke EPSCs, we delivered paired pulse test stimulation to dorsal root consisting of 2 synaptic volleys (500 μA, 0.1 ms) 400 ms apart at a frequency of 0.05 Hz to activate high-threshold afferent fibers (C-fibers), followed by a 0.1-ms 5-mV depolarizing pulse (to measure R series and R input). We monitored R series and R input and discarded cells if either of these values changed by more than 20%. The amplitudes of the first (P1) and the second (P2) EPSC were measured and the paired pulse ratio (PPR) was calculated as PPR = P2/P1.

Immunofluorescence

For spinal cord staining, adult mice (8–12 weeks old) were anesthetized with pentobarbital and perfused intracardially with 20 ml 0.1 M PBS (pH 7.4, 4 °C) followed with 25 ml of fixative (4% formaldehyde (vol/vol), 4 °C), as previously described (Han et al., 2013). Spinal cord was dissected from the perfused mice and post-fixed in fixative at 4 °C for 1 h. Then tissues were cryoprotected in 20% sucrose (wt/vol) for 24 h at 4 °C and were sectioned with Vibratome cryostat (Polysciences, Warrington, PA). The sections on slides were dried at 37 °C for 15 min, and fixed with 4% paraformaldehyde at room temperature for 10 min. Tyramide Signal Amplification (TSA) Systems (PerkinElmer, Waltham, MA) was used following the protocol provided. Rabbit polyclonal anti-BAM22 antiserum (1:500, ATSBIO, San Diego, CA, USA) in 1×TNB overnight at 4 °C followed by washing and incubation with secondary HRP-conjugated goat anti-rabbit IgG (1:500 in 1×TNB, Vector Laboratories, Burlingame, CA, USA) for 1 h. TSA cyanine 3 reagent was added for the amplification step.

Statistics

Data are presented as mean ± s.e.m. The number of mice analyzed is represented as *n*. Statistical comparisons were conducted by two-tailed, unpaired or paired Student's *t* test according to experimental design. Statistical significant difference was assumed at $P < 0.05$. Experiments were replicated biologically at least three times.

Results

Generation of humanized MrgprX1 mice

To establish a mouse model that resembles human Mrgpr signaling, we generated a bacterial artificial chromosome (BAC) transgenic *Mrgprx1* mouse line. Many *Mrgpr*s, such as mouse *Mrgpra3* and *Mrgprc11* and human *Mrgprx1*, are expressed only in subsets of small-diameter sensory neurons in DRG and trigeminal ganglia (Dong et al., 2001). In such a subset of sensory neurons, a certain cohort of ion channels and signal transduction pathways are present for Mrgpr to properly relay somatosensory information (Han et al., 2002; Wilson et al., 2011). To restrict the expression of *Mrgprx1* gene in the *Mrgpr*-expressing subset, we designed the construct so that *Mrgprx1* expression would be driven by the *Mrgprc11* promoter (Fig. 3.1A) because human *Mrgprx1* is considered most related to mouse *Mrgprc11* based on amino acid identity, ligand binding profiles, and expression patterns (Dong et al., 2001; Han et al., 2002; Lembo et al., 2002). The $Mrgprc11^{Mrgprx1}$ transgenic line was mated to the $Mrgpra3^{GFP\text{-}Cre}$ transgenic line in which the green fluorescent protein (GFP)-Cre fusion protein is driven by *Mrgpra3* promoter (Han et al., 2013). Because *Mrgpra3* and *Mrgprc11* are expressed in largely overlapping subsets of DRG neurons (Han et al., 2013), we were able to identify the neurons expressing MrgprX1 transgene for cellular study by intrinsic GFP fluorescence (Fig. 3.1C). Finally, we mated these lines with $Mrgpr\text{-}cluster\Delta^{-/-}$ mice, which have an 845-kilobase deletion that removes 12 endogenous *Mrgpr* genes (Liu et al., 2009) (e.g., *Mrgprc11* and *Mrgpra3*). The resulting $Mrgpr\text{-}cluster\Delta^{-/-}$; $Mrgprc11^{Mrgprx1}$; $Mrgpra3^{GFP\text{-}Cre}$ mouse line, which we call the "humanized MrgprX1 mouse model," allows us to study the role of MrgprX1 alone (Fig. 3.1B).

The expression of MrgprX1 receptor does not significantly alleviate hypersensitivity during persistent pain condition as revealed by formalin induced second-phase pain (Fig. 3.1D,E) and CFA induced persistent pain (Fig. 3.1F,G).

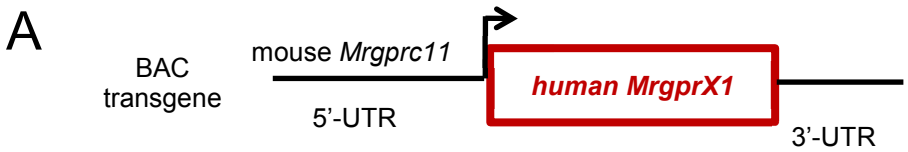

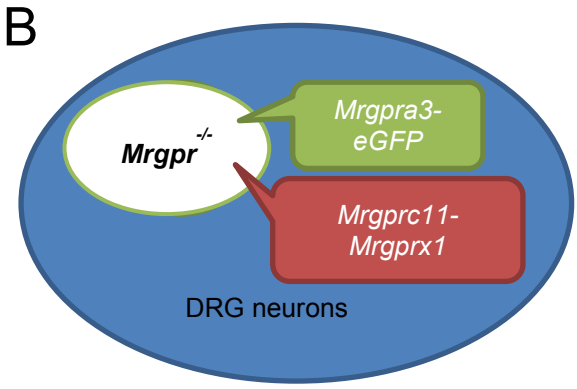

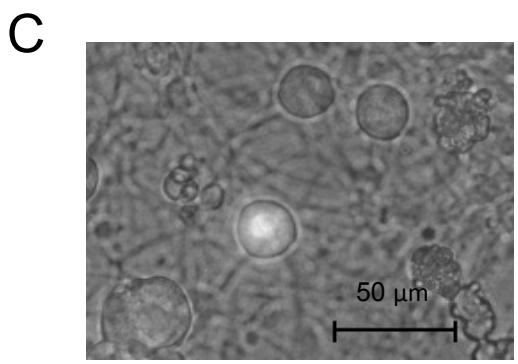

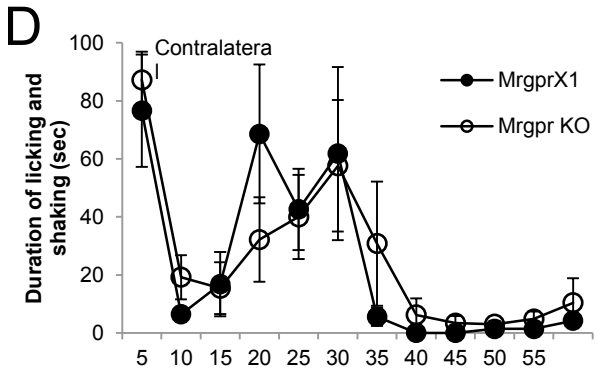

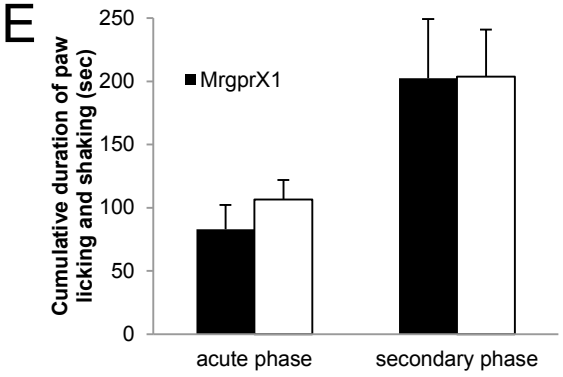

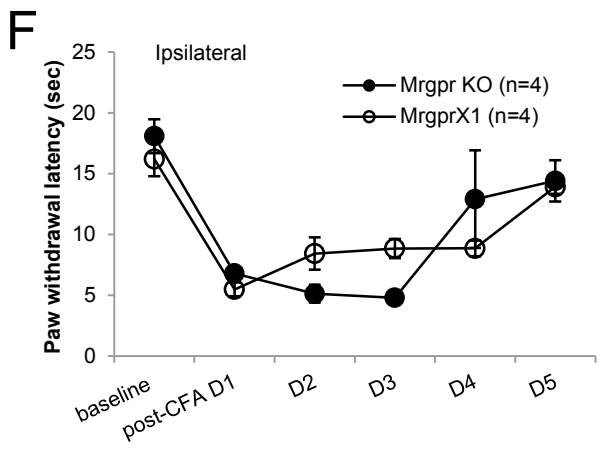

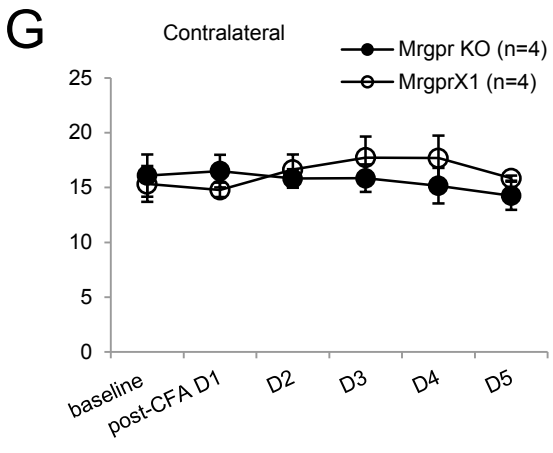

Figure 3.1 Generation of humanized MrgprX1 mouse line. (A) The BAC transgenic line expresses human *Mrgprx1* driven by mouse *MrgprC11* promoter. **(B)** *Mrgprc11*^{Mrgprx1} transgenic mice were mated with *Mrgpra3*$^{GFP\text{-}Cre}$ transgenic mice and then crossed into the *Mrgpr-clusterΔ*$^{-/-}$ background. Therefore, the *Mrgpra3*-GFP^{+} neurons, which are a small subset of all the DRG neurons, express human MrgprX1 but not mouse endogenous Mrgprs. **(C)** The brightfield image shows GFP^{+} neurons, which were used for electrophysiology experiments. **(D)** The second phase of formalin-induced pain was slightly, but not significantly, lower in humanized MrgprX1 mice than in *Mrgpr-clusterΔ*$^{-/-}$ (Mrgpr KO) mice. **(E)** The cumulative duration of licking and shaking post formalin injection into the hind paw in both phases are similar in the two genotypes. **(F)** Complete Freund's adjuvant (CFA)-induced thermal hypersensitivity was similar in humanized MrgprX1 and *Mrgpr-clusterΔ*$^{-/-}$ mice. **(G)** Thermal sensitivity of the uninjured contralateral paw was similar in both genotypes.

Activation of MrgprX1 inhibits high-voltage activated Ca^{2+} channels

To investigate whether activation of MrgprX1 also inhibits Ca^{2+} channels, we cultured acutely dissociated DRG neurons from humanized MrgprX1 mice and recorded Ca^{2+} current (I_{Ca}) in neurons labeled with *MrgprA3*-driven GFP. Every GFP-expressing neuron that we recorded responded to BAM8–22. We used a protocol that enabled us to record both low-voltage-activated (LVA) and HVA Ca^{2+} channels simultaneously, as shown in Fig. 3.2A (Chen and Ikeda, 2004). We noticed that in our recordings, all of the *Mrgpra3*-GFP^{+} neurons dominantly expressed HVA Ca^{2+} channel, very few LVA Ca^{2+} channel (Fig. 3.2A) (LVA I_{Ca} = -20.17 pA ± 2.57 pA , N = 35). We found that BAM8–22 inhibited HVA I_{Ca} and that ML382 significantly enhanced this inhibition (Fig. 3.2A). The inhibition by BAM8–22 was rapid and reversible (Fig. 3.2B). ML382 significantly increased inhibition of I_{Ca} by 0.5 μM BAM8–22. However, if the concentration of BAM8–22 was saturating (5 μM), ML382 was not able to further reduce I_{Ca} (Fig. 3.2A,C). The current inhibition was voltage-dependent. BAM8–22 shifted voltage dependency of the activation curve to more positive membrane potentials, which resulted in reduction of the channel open probability (Fig. 3.2D). ML382 shifted the activation curve even more in the positive direction in the presence of sub-saturating but not saturating concentrations of BAM8–22 (Fig. 3.2D). In the absence of BAM8–22, ML382 did not inhibit I_{Ca} (Fig. 3.2E) or shift the voltage dependency (Fig. 3.2F). The fact that ML382 enhanced BAM8–22 effect but did not act on MrgprX1 per se suggested that ML382 is an allosteric modulator of MrgprX1 and likely increases the binding affinity of BAM8–22.

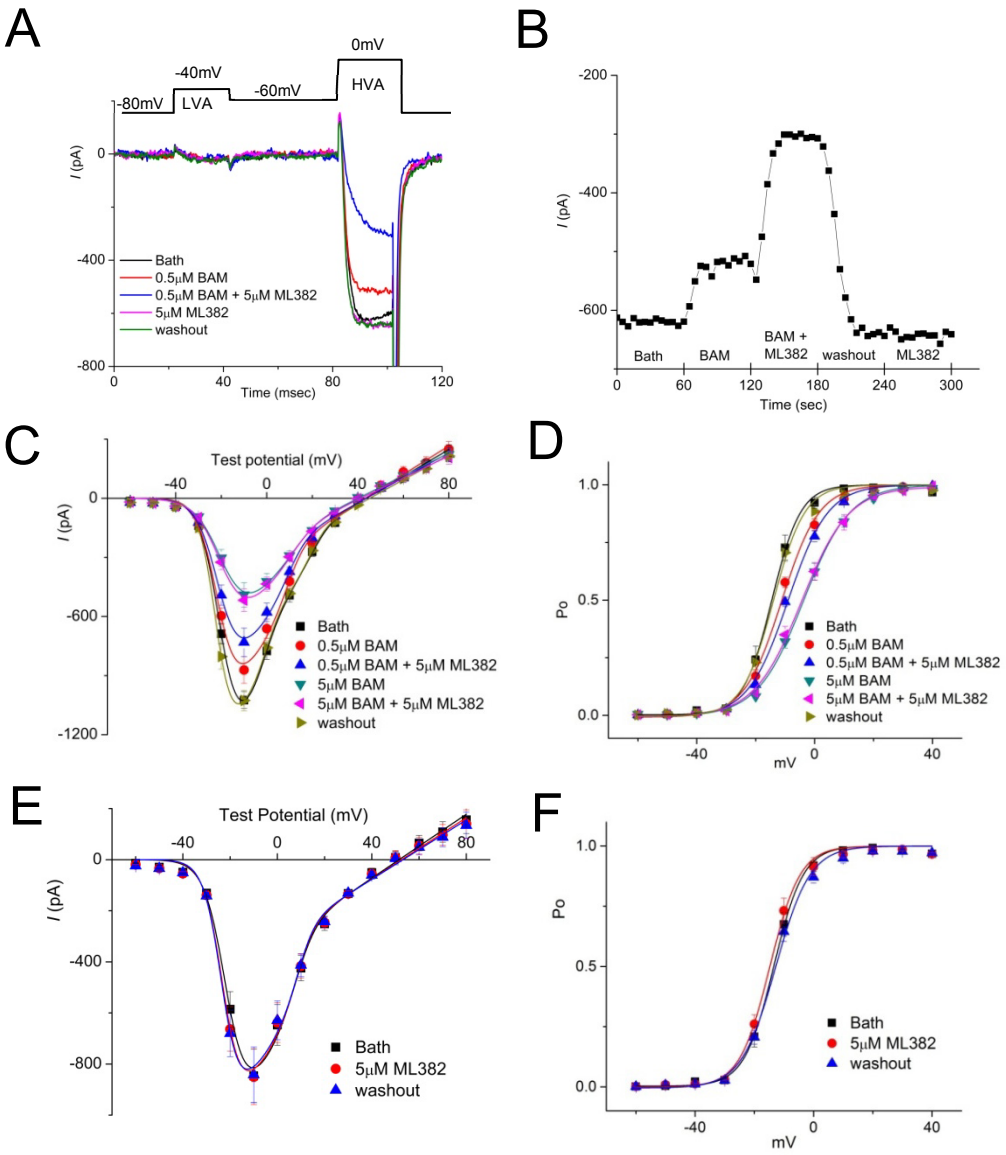

Figure 3.2 MrgprX1 induces inhibition of I_{Ca}. (A) A representative trace shows the protocol used to record current from low- and high-voltage-activated (LVA and HVA) Ca^{2+} channels. HVA I_{Ca} was inhibited by BAM8–22 (BAM) and significantly enhanced by ML382. ML382 alone did not inhibit HVA I_{Ca}. **(B)** A representative time course of the agonist effects on HVA I_{Ca} shows that the inhibition is rapid and reversible. **(C)** Current-voltage relation showing the inhibitory effect of BAM8–22 and ML382. **(D)** Open probability showing that BAM8–22 shifted the voltage dependency of the activation curve to more positive membrane potentials. ML382 alone did not inhibit I_{Ca} **(E)** or shift the voltage dependency **(F)**.

ML382 is a strong and selective positive allosteric modulator of MrgprX1

To confirm that ML382 modulates BAM8–22 binding affinity, we measured dose-response curves of BAM8–22 in the presence of different concentrations of ML382 in cultured DRG neurons from humanized MrgprX1 mice (see example trace without ML382 in Fig. 3.3A). In the absence of ML382, the EC_{50} for BAM8–22 inhibition of I_{Ca} was 0.66 ± 0.05 μM. In the presence of 0.1, 1, 10, and 30 μM ML382, BAM8–22 EC_{50} was reduced to 0.43 ± 0.02, 0.25 ± 0.02, 0.06 ± 0.01, and 0.08 ± 0.01 μM, respectively (Fig. 3.3B). A lower EC_{50} indicates higher binding affinity. This finding that ML382 dose-dependently increases BAM8–22 affinity demonstrates that ML382 is a positive allosteric modulator of MrgprX1. To quantify the potency of ML382, we applied a ternary complex model developed by De Lean et al. (De Lean et al., 1980) to estimate its cooperativity factor as well as its binding affinity (see METHOD). This model is needed to measure the binding affinity of ML382 because ML382 itself does not affect MrgprX1. Titrating ML382 in the presence of a sub-saturating concentration BAM8–22 is simplistic because ML382 affinity would change under the influence of BAM8–22 concentration when these two molecules exhibit allostery. In addition, the ternary complex model provides a factor known as α, which can be used as an indicator to quantify the magnitude of this allosteric regulation. We found the EC_{50} of ML382 to be 3.2 ± 1.7 μM and the α value to be 11.5 ± 1.3. The fact that α was much larger than 1 suggests that ML382 is a very potent positive allosteric modulator (Fig. 3.3C). We also cultured DRG neurons from wild-type mice that express MrgprA3-promoter–driven GFP in order to test the effect of ML382 on MrgprC11, a close mouse Mrgpr member of MrgprX1 that can also be activated by BAM peptides. We found that ML382 did not enhance BAM8–22 inhibition of current (Fig. 3.3D). Together these data suggest that ML382 is a very potent and selective allosteric modulator of MrgprX1.

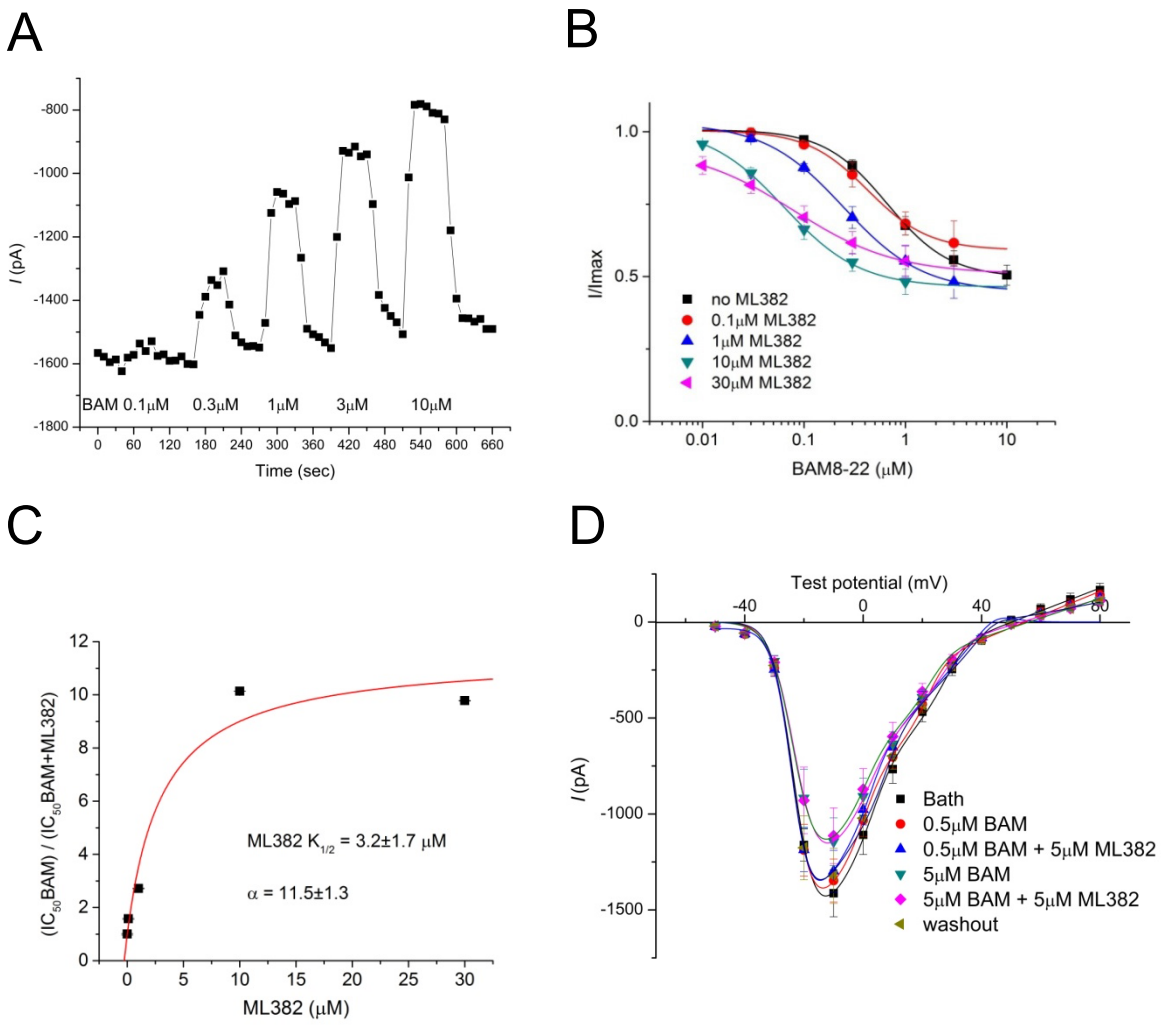

Figure 3.3 Quantification of the potency of ML382 as a positive allosteric agonist. (A) A representative time course shows the protocol used to measure the dose-response curve of BAM8–22-induced inhibition of HVA I_{Ca}. **(B)** EC_{50} of BAM8–22 in the presence and absence of different concentrations of BAM8–22. **(C)** Equation used to calculate the EC_{50} and α value of ML382. **(D)** ML382 did not enhance BAM8–22 inhibition of HVA I_{Ca} through mouse MrgprC11.

BAM8–22 predominantly inhibits N-type Ca^{2+} channel in a partially voltage-dependent manner and is sensitive to Gi blocker

DRG neurons express at least three types of HVA Ca^{2+} channels, namely N-, P/Q-, and L-type (Fox et al., 1987; Yusaf et al., 2001). Each can be isolated by a specific blocker (Catterall, 2000; Gribkoff, 2006). We found that all three types of calcium channels are present in *Mrgpra3*-GFP–labeled neurons (Fig. 3.4A,B). To identify which calcium channel is the downstream target of MrgprX1, we used ω-conotoxin GVIA, ω-agatoxin, and nimodipine to block N-type, P/Q-type, and L-type HVA Ca^{2+} channels, respectively. We applied each blocker individually and tested BAM8–22-induced current inhibition. Application of 1 μM ω-conotoxin GVIA decreased BAM8–22-induced inhibition from 52.2% to 10.0%, suggesting that the N-type calcium channel is a major target of MrgprX1 (Fig. 3.4C,F). In contrast, 0.5 μM ω-agatoxin and 10 μM nimodipine altered the effect of BAM8–22 to 43.5% and 57.4%, respectively (Fig. 3.4D–F). ML382 was not able to divert the downstream effect by acting at another HVA when N-type HVA was blocked by ω-conotoxin GVIA (Fig. 3.4C–E).

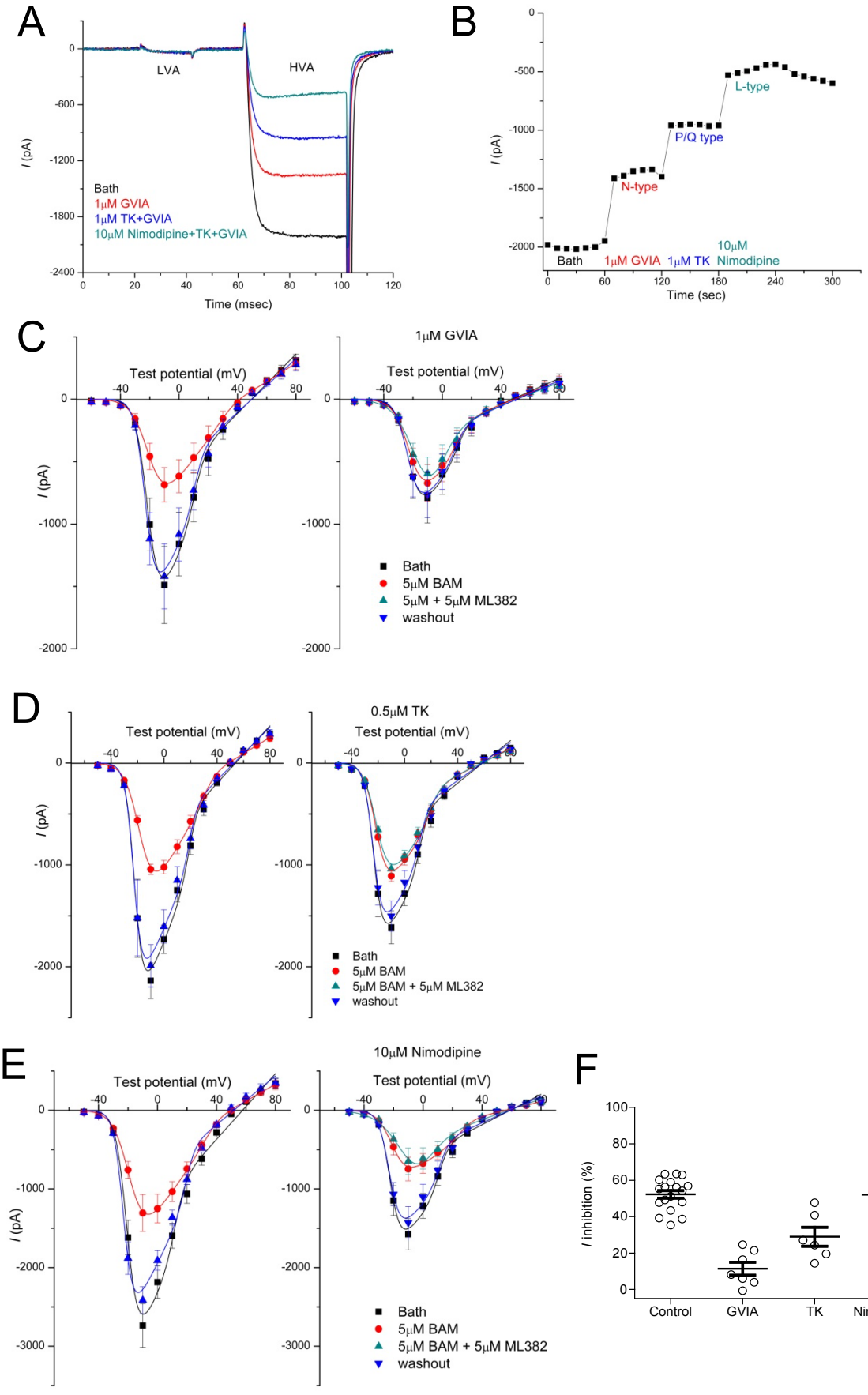
A
LVA
HVA
Bath
1μM GVIA
1μM TK+GVIA
10μM Nimodipine+TK+GVIA
I (pA)
Time (msec)
B
L-type
P/Q type
N-type
Bath
1μM GVIA
1μM TK
10μM Nimodipine
I (pA)
Time (sec)
C
1μM GVIA
Test potential (mV)
I (pA)
Bath
5μM BAM
5μM + 5μM ML382
washout
D
0.5μM TK
Test potential (mV)
I (pA)
Bath
5μM BAM
5μM BAM + 5μM ML382
washout
E
10μM Nimodipine
Test potential (mV)
I (pA)
Bath
5μM BAM
5μM BAM + 5μM ML382
washout
F
I inhibition (%)
Control
GVIA
TK
Nimodipine

Figure 3.4 MrgprX1 predominantly inhibits N-type HVA Ca^{2+} channel. (A) A representative trace shows the different components of high-voltage-activated (HVA) I_{Ca} separated by blockers. **(B)** A representative time course of the effect of channel blockers on HVA I_{Ca} shows that the inhibition is rapid and steady. **(C)** A graph of the current-voltage relationship shows that ω-conotoxin GVIA (GVIA for short in figures) abolished 90% of BAM8–22-induced current inhibition (n = 7 neurons). ML382 did not divert the downstream effect by acting at another HVA channel. **(D–E)** Current-voltage relationship graphs also show that ω-agatoxin TK (TK for short in figures) abolished 40% of BAM8–22-induced current inhibition (n = 6 neurons, **D**) and that nimodipine abolished 50% of BAM8–22-induced current inhibition (n = 5 neurons, **E**). **(F)** Amplitude of BAM8–22-induced current inhibition in the presence of different Ca^{2+} channel blockers, normalized by baseline level of HVA I_{Ca} in the same neuron without blockers or BAM8–22. ***P < 0.001, *P < 0.05 vs control (paired Student's t-test).

G-protein-mediated inhibition of N-type calcium channels is often coupled to the pertussis toxin (PTX)-sensitive $G_{i/o}$ pathway (Chen and Ikeda, 2004; Raingo et al., 2007) and involves G$\beta\gamma$ binding to the intracellular loop in a voltage-dependent manner (Hille et al., 1995; Herlitze et al., 1996; Qin et al., 1997). To further identify downstream G-protein pathways, we used PTX, cholera toxin (CTX), and U73122 to differentiate three types of G-protein signaling, namely $G_{i/o}$, G_s, and $G_{q/11}$-phospholipase C. We found that pretreatment with 2 µg/mL PTX completely abolished BAM8–22-induced inhibition (from 50.2% to 1.5%; Fig. 3.5A, D). In contrast, pretreatment with 2 µg/mL CTX or 5 µg/mL U73122 reduced BAM8–22-induced inhibition to only 49.8% and 34.3%, respectively (Fig. 3.5B–D). To investigate the role of G$\beta\gamma$ binding, we examined the effect of BAM8–22 with a sandwich protocol, a pair of activation pulses with a strong depolarizing intermediate pulse (Fig. 3.5E) (Herlitze et al., 1996; Raingo et al., 2007). If the effect of BAM8–22 is mediated by G$\beta\gamma$ binding, the strong depolarizing prepulse will dessociate G$\beta\gamma$ from N-type calcium channel and reverse the inhibition. We found that the strong depolarizing prepulse reversed 50% of BAM8–22-induced inhibition (Fig. 3.5F). The voltage dependent activation curve (PV curve) showed that this voltage protocol fully reversed the voltage dependence of the channel (Fig. 3.5G); therefore the remaining inhibition was voltage-independent. These results confirmed that the analgesic effect of BAM8–22 is mediated by $G_{i/o}$-sensitive G$\beta\gamma$ binding of N-type calcium channel and also suggested the existence of a G$\beta\gamma$-independent pathway (Fig. 3.5H).

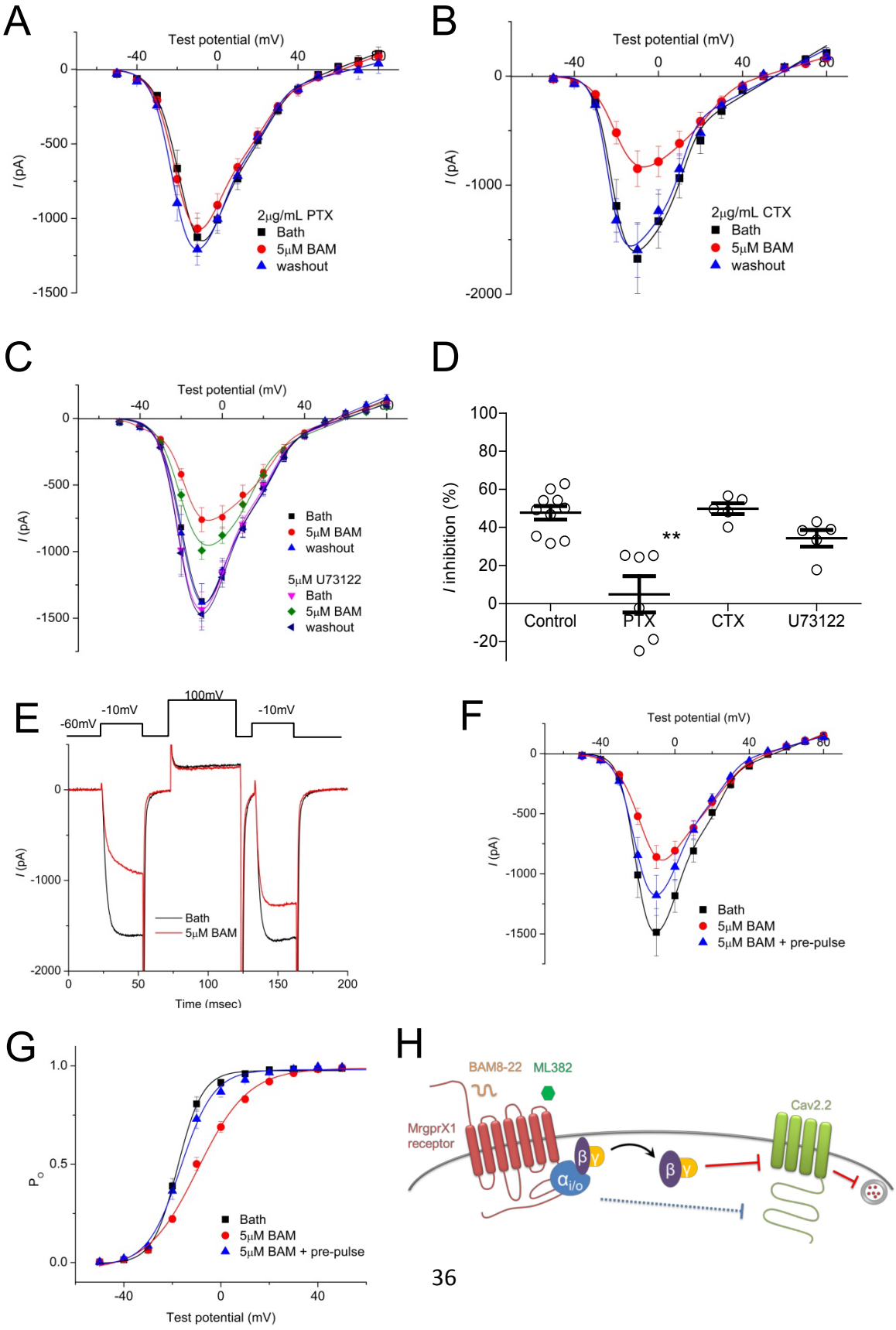
A
Test potential (mV)
I (pA)
2μg/mL PTX
Bath
5μM BAM
washout
B
Test potential (mV)
I (pA)
2μg/mL CTX
Bath
5μM BAM
washout
C
Test potential (mV)
I (pA)
Bath
5μM BAM
washout
5μM U73122
Bath
5μM BAM
washout
D
I inhibition (%)
**
Control
PTX
CTX
U73122
E
-60mV
-10mV
100mV
-10mV
I (pA)
Bath
5μM BAM
Time (msec)
F
Test potential (mV)
I (pA)
Bath
5μM BAM
5μM BAM + pre-pulse
G
P_o
Bath
5μM BAM
5μM BAM + pre-pulse
Test potential (mV)
H
BAM8-22
ML382
MrgprX1 receptor
Cav2.2

Figure 3.5 MrgprX1 mediates $G_{i/o}$-sensitive G$\beta\gamma$ binding to N-type calcium channel. (A) Overnight pretreatment of neurons with pertussis toxin (PTX) completely abolished BAM8–22-induced current inhibition (*n* = 6 neurons). **(B)** Overnight pretreatment with cholera toxin (CTX) did not produce a notable effect on BAM8–22-induced inhibition (*n* = 5 neurons). **(C)** Acute perfusion with U73122 (3 minutes) did not produce a notable effect on BAM8–22-induced inhibition (*n* = 5 neurons). **(D)** Amplitude of BAM8–22-induced inhibition in the absence (control) and presence of different blockers, normalized by pre-BAM8–22 baseline of the same neuron. Only the PTX-treated group showed a significant decrease compared to control. $^{**}P < 0.01$ vs control. **(E)** A representative trace shows the sandwich protocol used to relieve G$\beta\gamma$ binding to the HVA Ca^{2+} channels. **(F)** A graph of the current-voltage relationship shows that the depolarizing prepulse reversed 50% of BAM8–22-induced inhibition (*n* = 6 neurons). **(G)** Open probability shows that the depolarizing prepulse fully reversed the voltage dependence of the channel. **(H)** A schematic model of MrgprX1-mediated HVA I_{Ca} inhibition. BAM8–22 activates MrgprX1, which predominantly inhibits N-type calcium channels and reduces neurotransmitter release. This inhibition is contributed to in part by G$\beta\gamma$ binding. $G\alpha_{i/o}$ might also be involved. ML382 is a selective MrgprX1 allosteric agonist that can boost BAM8–22-induced current inhibition by increasing its potency. Paired Student's *t*-test was used for statistical analysis.

BAM22 peptide at spinal cord dorsal horn is upregulated during persistent pain conditions

We next investigated whether endogenous BAM peptides are secreted at the central terminal as a physiological mechanism to counteract persistent pain. We stained for BAM22 peptide immunoreactivity using anti-BAM22 antibody and compared the injured and uninjured sides of spinal cord dorsal horn (L4-L5) from humanized MrgprX1 mice 2 days after injection with complete Freund's adjuvant (CFA) or 3 weeks after chronic constriction injury (CCI) of the sciatic nerve. BAM22 immunoreactivity appeared at superficial layers (laminae I–II) (Chen et al., 2008) and was elevated on the injured side (Fig. 3.6A-B). The antibody was validated by pre-absorbed the anti-BAM22 antiserum with 10^{-6} M BAM22, resulting in the complete absence of BAM22 signal (Fig. 3.6C,D).

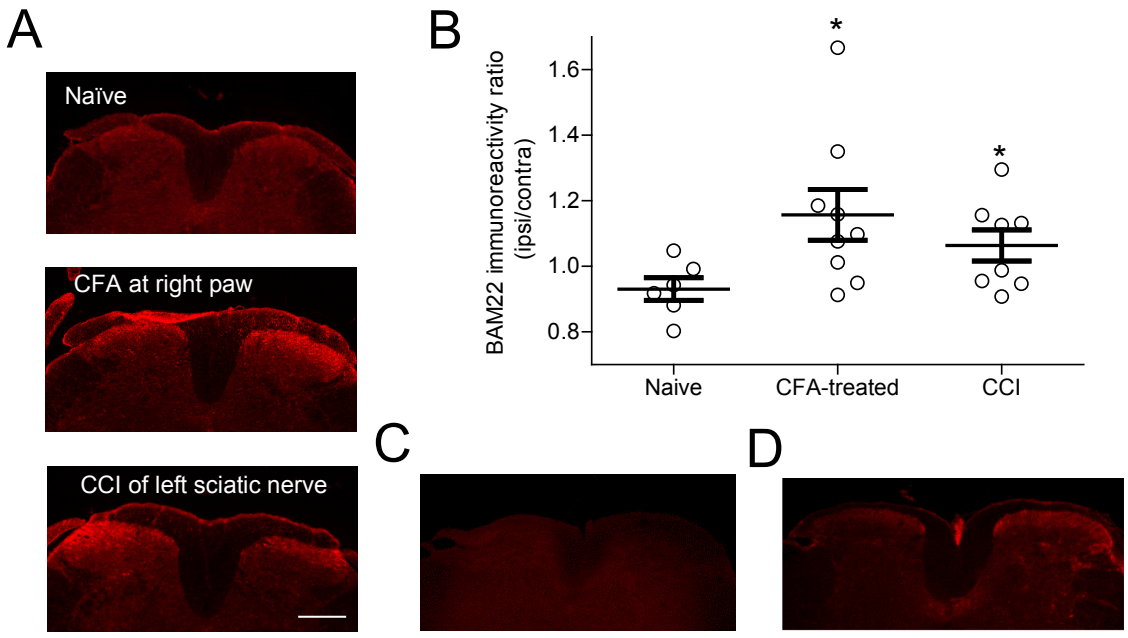

Figure 3.6 BAM22 immunoreactivity increases during chronic pain condition at spinal cord dorsal horn. (A) Representative staining of L4-L5 spinal cord dorsal horn from naïve mice and mice subjected to complete Freund's adjuvant (CFA) or chronic constriction injury (CCI). **(B)** Quantification of BAM22 immunoreactivity. **P* < 0.05 vs naïve, repeated in5 animals for each condition. **(C)** The anti-BAM22 antiserum was pre-absorbed with 10^{-6} M BAM22, resulting in the absence of BAM22 signal. **(D)** A continuous section of the spinal cord form the same animal was stained with anti-BAM22 antibody that was not pre-absorbed. The BAM22 immunoreactivity was seen on the superficial layers of dorsal horn. The right side has a higher level of signal, which was ipsilateral to the CFA treatment on the hind paw. Scale bar represents 500 μm.

We then quantified the level of BAM22 in mouse spinal cords by a highly sensitive targeted mass spectrometry (MS) approach, termed liquid chromatography-selected reaction monitoring (LC-SRM). Basically, the BAM22 peptide together with other molecules were extracted from the spinal cords, trypsinized, and resolved by reverse phase LC. The eluted BAM22 $_{8\text{-}19}$ peptide (i.e. VGRPEWWMDYQK) was ionized and transferred into MS that was operated in a mode of selected reaction monitoring (SRM). In SRM, the BAM22 peptide ion was separated from other co-eluting ions, and then fragmented to generate specific product ions, which indicated the intensity of BAM22 in the original samples. In such a targeted analysis, we first defined the precursor ion and fragmented MS/MS pattern of the BAM22 $_{8\text{-}19}$ peptide using a synthetic peptide (Fig. 3.7A), then measured the absolute level of BAM22 peptide in CFA treated spinal cord (247 ± 2 femtomoles per spinal cord, 6.8 nM, Fig. 3.7B). Whereas BAM22 was quantified by three different product ions, the specificity of this analysis was strongly supported by identical features between the endogenous BAM22-derived peptide and its synthetic counterpart, with respect to precursor ion, LC retention time, and multiple product ions. Finally, based on five product ions, we found that CFA treatment induced an increase (46.0 ± 3.6 %) of the BAM22 level in the spinal cord (Fig. 3.7C). The level of BAM22 in skin was not detectable in neither the control mice nor CFA-treated mice.

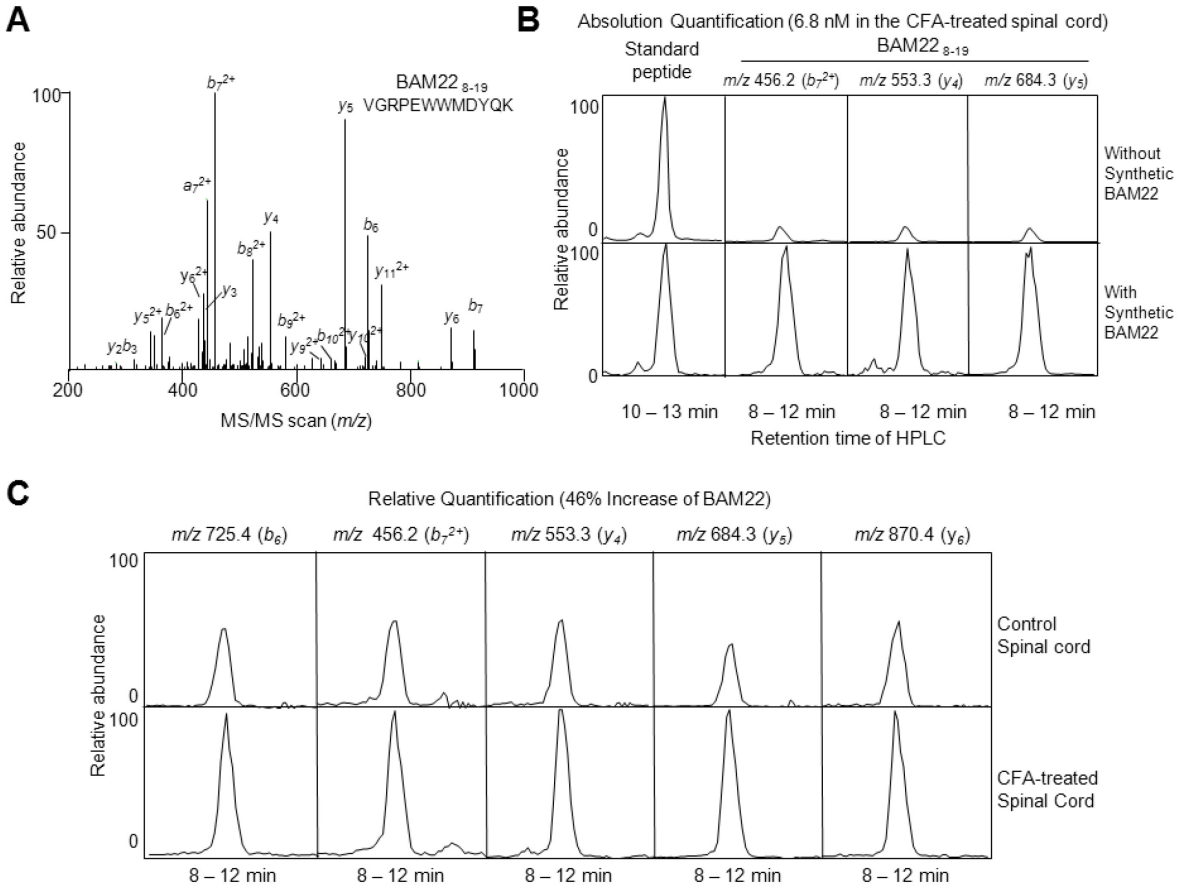

Figure 3.7 Quantification of BAM22 peptide in mouse spinal cords by mass spectrometry. **(A)** The MS/MS spectrum of triply charged BAM22 $_{8-19}$ tryptic peptide (VGRPEWWMDYQK, 532.3 *m/z*). **(B)** Absolute quantitative analysis of BAM22 $_{8-19}$ (6.8 nM) in the CFA treated mouse spinal cord by LC-SRM, based on peak area difference in the CFA-treated spinal cord samples before and after adding 250 femtomoles of synthetic BAM22. Three product ions were monitored. In addition, the run-to-run variation was corrected by spiking in 100 femtomoles of another synthetic peptide (TLSDYNIQKESTLHLVLR, triply charged precursor ion of 710.8 *m/z*) as external standard. **(C)** Comparison of the BAM22 expression level between control and CFA treated mouse spinal cords shows that CFA treatment induced an increase (46.0 ± 3.6 %) of the BAM22 level. Five transitions were monitored for relative quantification.

Activation of MrgprX1 blocks presynaptic functions in the spinal cord dorsal horn

Because the central projections of Mrgpr^{+} C-fibers terminate in superficial dorsal horn (Han et al., 2013; He et al., 2014), we continued testing whether MrgprX1 acts at central terminals by recording from substantia gelatinosa (SG) neurons (lamina II) in lumbar spinal cord slices (L4-L5 segments) from mice with CFA-induced inflammation of the hind paw. Evoked excitatory presynaptic currents (eEPSCs) were recorded after the application of high-intensity paired-pulse stimulation (500 μA, 0.1 ms, 400 ms apart, 3 tests/min) at the dorsal root, which activates high-threshold afferent fibers (C-fibers) (Li et al., 2014). In 10 of 18 SG neurons (55.6%), 0.5 μM BAM8–22 inhibited eEPSCs. This inhibition was significantly enhanced by ML382 (Fig. 3.8A,B). In contrast, BAM8–22 was not able to inhibit eEPSCs in the SG neurons from *Mrgpr-cluster*$\Delta^{-/-}$ mice in the presence or absence of ML382. ML382 alone did not have any effect on SG neuron eEPSCs from either humanized MrgprX1 or *Mrgpr-cluster*$\Delta^{-/-}$ mice.

To examine further whether such inhibition of postsynaptic response involves a decrease in presynaptic release of excitatory neurotransmitters, we used a paired pulse test stimulation of dorsal root to quantify paired pulse ratio (PPR) in the presence or absence of BAM8–22 or ML382. A pair of two synaptic volleys (500 μA, 0.1 ms) was applied at a frequency of 0.05 Hz. The PPR is defined as the 2nd eEPSCs (P2) over the the 1st eEPSC (P1) evoked by these two pulse. The change in PPR can be used to indicate that the inhibition of postsynaptic response by a drug may involve presynaptic inhibition of the release of excitatory neurotransmitters (Heinl et al., 2011; Li et al., 2014). We found that 0.5 μM BAM8–22 with 5 μM ML382 increased PPR significantly, suggesting presynaptic modulation of eEPSCs. ML382 alone did not affect PPR (Fig. 3.8C,D). Importantly, this phenomenon was observed only in slices from humanized MrgprX1 mice, not in those from *Mrgpr-cluster*$\Delta^{-/-}$ mice, supporting the idea that this presynaptic modulation is MrgprX1-dependent.

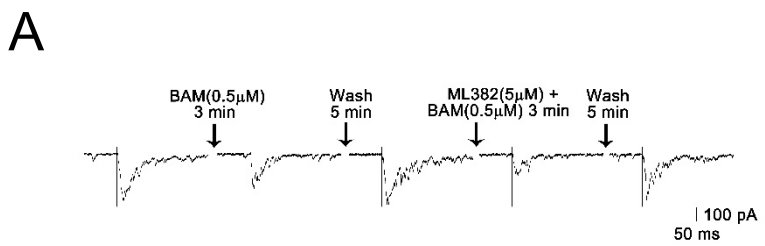
A
BAM(0.5μM)
3 min
Wash
5 min
ML382(5μM) +
BAM(0.5μM) 3 min
Wash
5 min
100 pA
50 ms

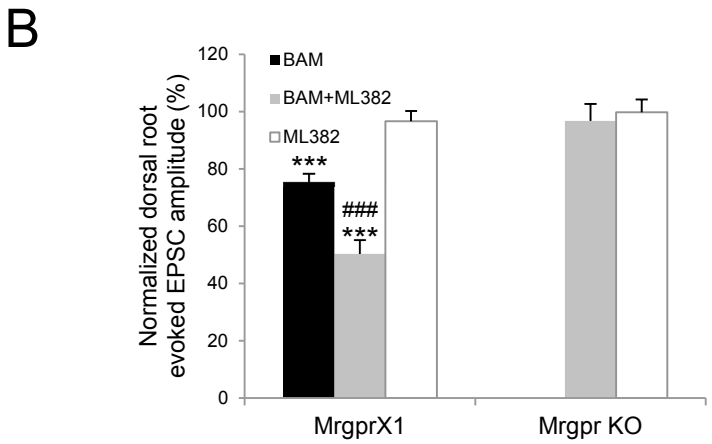
B
BAM
BAM+ML382
ML382
Normalized dorsal root evoked EPSC amplitude (%)
120
100
80
60
40
20
0
***
###
***
MrgprX1
Mrgpr KO

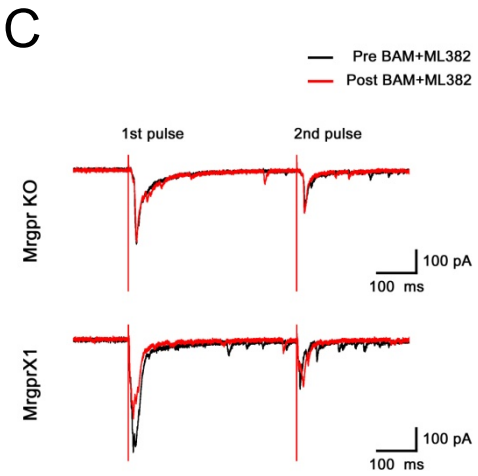
C
Pre BAM+ML382
Post BAM+ML382
1st pulse
2nd pulse
Mrgpr KO
100 pA
100 ms
MrgprX1
100 pA
100 ms

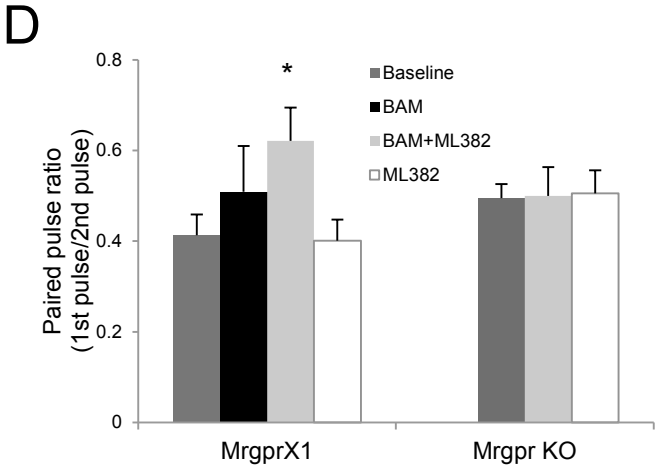
D
Baseline
BAM
BAM+ML382
ML382
Paired pulse ratio (1st pulse/2nd pulse)
0.8
0.6
0.4
0.2
0
*
MrgprX1
Mrgpr KO

Figure 3.8 MrgprX1 activation blocks presynaptic functions in spinal cord dorsal horn. (A) Representative trace of evoked EPSCs in the presence of agonists in substantia gelatinosa (SG) neurons from CFA-treated humanized MrgprX1 mice and *Mrgpr-clusterΔ*$^{-/-}$ mice (Mrgpr KO). **(B)** BAM8–22 (0.5 μM) significantly decreased evoked EPSCs of SG neurons (*n* = 10 neurons). The inhibition was enhanced by ML382 (5 μM; *n* = 10 neurons). ML382 alone did not affect evoked EPSCs (*n* = 7 neurons from humanized MrgprX1 mice, *n* = 11 neurons from Mrgpr KO mice). Neurons from Mrgpr KO mice did not respond to BAM8–22 or ML382 (*n* = 8 neurons). ***P < 0.001 vs pre-drug value; $^{###}P$ < 0.001 vs BAM8–22. **(C)** Representative traces of evoked EPSCs in response to high-intensity, paired-pulse stimulation (500 μA, 0.1 ms, 400 ms interval) before (black) and 5 minutes after (red) bath application of BAM8–22 and ML382 in SG neurons from CFA-injected humanized MrgprX1 mice and Mrgpr KO mice. **(D)** In the MrgprX1 group, BAM8–22 and ML382 increased the paired pulse ratio. *P < 0.05 vs pre-drug baseline. Paired Student's *t*-test was used for statistical analysis.

Discussion

In summary, our electrophysiology data indicated that ML382 enhanced the ability of MrgprX1 to inhibit high-voltage activated Ca^{2+} channels by increasing the potency of BAM8–22. Endogenous MrgprX1 agonist BAM22 is up-regulated at spinal cord dorsal horn under chronic pain condition. Activation of MrgprX1 by BAM8–22 reduces neurotransmitter release by inhibiting N-type voltage-activated calcium current through PTX sensitive Gi/o pathway. Together, the evidence unveils the endogenous negative feedback machinery of MrgprX1 as a target of endogenous peptide BAM22 to tune down central sensitization during chronic pain.

Our electrophysiogical study showed that activation of MrgprX1 inhibits HVA I_{Ca}, consistent with the results of a previous study that used heterologously expressed MrgprX1 in superior cervical ganglion and DRG neurons (Chen and Ikeda, 2004). Interestingly, that study showed that MrgprX1 couples to HVA but not LVA (Chen and Ikeda, 2004). Similarly, the *Mrgpra3*-GFP^+ neurons that we recorded do not possess an LVA component. This finding suggests that the MrgprX1 pathway is highly preserved in a specific subpopulation of peripheral neurons. It also supports our experimental design to drive *MrgprX1* gene with the mouse *MrgprC11* in order to restore a physiologically relevant expression pattern.

We found that MrgprX1 inhibits mainly N-type Ca^{2+} channels, similar to what we found with MrgprC11 activation (Li et al., 2014). N-type HVA Ca^{2+} channels can bind to the protein SNAP-25 and syntaxin-1A and couple the opening of the channels to vesicle fusion, causing neurotransmitter release into the spinal cord dorsal horn (Catterall, 2000; Yusaf et al., 2001; McGivern and McDonough, 2004; Gribkoff, 2006). N-type HVA channel is also an important target for opioid inhibition of pain through the $G_{i/o}$ pathway (Hescheler et al., 1987; Kaneko et al., 1994; Moises et al., 1994; Bourinet et al., 1996), indicating again that Mrgprs may be an endogenous inhibitory pathway parallel to opioid system.

Our electrophysiological study also confirmed that BAM8–22 inhibition of HVA I_{Ca} is partially voltage-dependent (Chen and Ikeda, 2004). A strong depolarizing pulse reversed 50% of the inhibition mediated by BAM8–22. This finding suggests partial involvement of G$\beta\gamma$ binding. Unlike Chen and Ikeda (Chen and Ikeda, 2004), we observed that overnight pretreatment with PTX completely abolished BAM8–22 inhibition of HVA I_{Ca}, suggesting that BAM8–22 activates MrgprX1 and triggers $G_{i/o}$-sensitive G$\beta\gamma$ binding to N-type calcium channels. The discrepancy between our data and theirs suggests that MrgprX1 receptor might activate different G protein pathways in different subpopulations of DRG neurons. Therefore we studied MrgprX1 receptor in *Mrgpra3*-GFP$^+$ neurons.

The inhibition of N-type HVA I_{Ca} in DRG neurons caused a decrease in neurotransmitter release into spinal cord dorsal horn neurons, as we observed reduced eEPSCs in the presence of BAM8–22 and ML382. We confirmed that this effect occurs presynaptically at the central terminal of *Mrgpra3*-GFP$^+$ DRG neurons, as PPR of SG neurons increased. Though *Mrgprc* promoter is expressed in ~10% of mouse DRG neurons, over half of SG neurons in the dorsal horn from CFA-treated humanized MrgprX1 mice responded to BAM8–22, suggesting that Mrgpr$^+$ DRG central termini form broad branches and arborize extensively in superficial dorsal horn to contact multiple postsynaptic neurons (Li et al., 2014).

ML382 was unable to enhance the inhibition of HVA I_{Ca} by BAM8–22 in MrgprC11-expressing DRG neurons from wild-type animals. MrgprX1 and MrgprC11 exhibit considerable difference in drug profile though they share 54% amino acid identity (Han et al., 2002). Species differences across Mrgprs are the main reason that many agonists have been reported for MrgprX1 but only a few were tested for *in vivo* functions (Lembo et al., 2002; Sikand et al., 2011; Wen et al., 2015). Thus, our humanized MrgprX1 mouse model provides a unique rodent platform that could be used to screen compounds against the human MrgprX1 receptor.

CHAPTER 4: ML382 INHIBITS PERSISTENT PAIN BEHAVIORALLY

Introduction

Nociceptors are the subpopulation of peripheral nerve fibers that detect harmful irritation such as intense thermal, mechanical or chemical stimuli (Basbaum and Jessell, 2000). Pain sensation is not recognized as a hard wired system, but rather a highly plastic one with the engagement of molecules and circuits (Basbaum et al., 2009). The nociceptors peripherally innervate the body (DRG neurons) and the face (trigeminal ganglion) and centrally relay information into the spinal cord dorsal horn. The nociception information is then ascended through spinothalamic tract into the brain (including thalamus, somatosensory cortex, midbrain, etc.). Modulation and integration happens at each of the above steps Therefore human sensation of pain is plastic and human experience of pain is multidimensional which comprises sensory, affective and cognitive aspects (Navratilova et al., 2013). It facilitates not only withdrawal and self-guarding from damaging situation but also learning process to avoid similar harmful situation in the future (Cox et al., 2010). Though pre-clinical research largely focuses on the molecular and cellular mechanism of the sensory aspect of evoked or persistent pain, the other aspects also need to be take into consideration during drug development, especially the affective aspect which is reported to be the most bothersome to human patients with ongoing persistent pain (Fields, 1999; Fields, 2007). Though difficult to be measured directly as the pain sensory behaviors in nonverbal animals, the affective/aversive aspect has been assessed by pain researchers using operant learning behavior. The principle is that the animals are motivated to avoid pain and incline to relief from ongoing pain, and thus allows researchers to evaluate avoidance from painful situation and reward from the termination of ongoing pain.

After demonstrating that the MrgprX1 receptor and endogenous orthosteric agonist BAM peptide function at the central terminal, we aimed to verify whether the allosteric modulator ML382 is able to produce analgesic effect in persistent pain conditions. We evaluated the relief of pain sensation for evoked pain and the affective/aversive effect caused by ML382.

Methods

Chronic pain models

Inflammation was induced by injecting the hind paw of mice subcutaneously with 6 μL of 50% CFA solution in saline (Guan et al., 2010). Pain response change was evaluated 24–48 hours after injection.

Neuropathic pain was induced by CCI of the sciatic nerve as previously described (He et al., 2014). Mice were anesthetized by inhalation of 2% isoflurane delivered through a nose cone. The left sciatic nerve at the middle thigh level was separated from the surrounding tissue and loosely tied with three nylon sutures (9-0 nonabsorbable monofilament, S&T AG, Neuhausen, Switzerland). The ligatures were approximately 0.5 mm apart.

Behavioral studies

Behavioral assays were performed by experimenters blind to genotype. The mice used in the tests were backcrossed to C57Bl/6 mice for at least 10 generations and were 2- to 3-month-old (20–30 g) males.

Intrathecal injection was performed as previously described (Guan et al., 2010). Briefly, ML382 was dissolved in DMSO to 50 mM, suspended in 0.9% saline to the desired working concentration, and injected into the intrathecal space under brief isoflurane (1.5%) anesthesia. A 30-gauge, 0.5-inch needle connected to a 50-μL syringe was inserted into one side of the L5 or L6 spinous process and moved carefully forward to the intervertebral space. A tail flick indicated that the tip of the needle was inserted into the subarachnoid space. The needle was removed after administration of 10–12 μL of drug solution.

One day before the formalin test, mice were acclimated to the environment for 1 hour. On the day of test, 7 μL of 2% formalin in saline was injected into the plantar region of one hind paw.

Spontaneous pain behavior (licking and twitching) was recorded for 60 minutes (Guan et al., 2010).

The Hargreaves test was performed as described in Han et al. (2013). Mice were placed under a transparent plastic box (4.5 × 5 × 10 cm) on a glass floor. Infrared light was delivered through the glass floor to the hind paw. After acclimatization sessions, the latency for the animal to withdraw its hind paw was measured.

For the conditioned place preference test, humanized MrgprX1 and *Mrgpr-clusterΔ*$^{-/-}$ mice underwent CCI of the left sciatic nerve. On day 7 after CCI, both naïve and nerve-injured animals were habituated (30 minutes/day) in an automated 3-chamber box to which they had access to all chambers. The two larger chambers of this apparatus contained distinct visual (vertical stripes vs. triangular shapes) and tactile (smooth floor vs. grooved floor texture) cues. The third, smaller chamber was interposed between the other two and was devoid of overt spatial cues. On the pre-conditioning day (day 11 post-CCI), behavior was video recorded for 15 minutes while the mice were again free to explore all 3 chambers. The results were used to quantify any basal chamber preference or aversion in individual mice. In keeping with a previous study (King et al., 2009), animals that spent more than 80% (> 720 seconds) or less than 20% (< 120 seconds) of the total time in any given chamber were eliminated from further testing. The next day (day 12 post-CCI), animals received a lumbar puncture injection of vehicle (saline, 10–12 μL, i.th.) under anesthesia and 10 minutes later were placed in one of the conditioning chambers for 45 minutes. Four hours later, the same animals received a lumbar puncture injection of ML382 (250 μM, 10-15 μL) and 10 minutes later were restricted to the opposite conditioning chamber for 45 minutes. On the post-conditioning test day (day 13 post-CCI), animals were placed in the same 3-chamber box with access to all chambers but received no injection. Their behavior was recorded for 15 minutes and used to analyze chamber preference or aversion. Data were pooled from 7 groups of mice, each containing humanized MrgprX1 and *Mrgpr-clusterΔ*$^{-/-}$ nerve-injured and naive animals. Pairing of ML382 or vehicle with a given chamber was counterbalanced between groups. For

each treatment group, we compared time spent in each chamber during pre- and post-conditioning days by paired *t*-test to determine if conditioned place aversion or preference was present. An increase in post-conditioning time spent in the ML382-paired chamber, as compared with pre-conditioning time in the same chamber, indicated conditioned place preference. In addition, difference scores were calculated as: (Post-conditioning time – Pre-conditioning time).

For itch behavioral study, mice had been acclimatized one day before test. BAM8–22 or ML382 was injected subcutaneously into the nape of the neck (50 μL), intraperitoneally (100 μL), or intrathecally (10-12 μL). Behavioral responses were video recorded for 30 minutes. The video recording was subsequently played back in slow motion, and an investigator counted the number of bouts of scratching with the hind paw around the injection site.

For motor function test, we used the rotarod test to evaluate whether central administration of ML382 affects motor function as described in Han et al. (2013). All animals were brought to the behavior room 10–20 minutes before the test. The mice habituated in the rotarod apparatus (Rotamex, Columbus Instruments) at a constant speed of 4 rpm for 10 minutes 3–5 times on day 1. Then, on day 2, they received three acceleration training sessions separated by 20 minutes. Speeds increased from 4 rpm to 40 rpm (with a 4.0-rpm increase every 30 seconds). On day 3, they received three trials before drug administration (in the same acceleration mode as day two). Then ML382 was applied intrathecally without isoflurane. The mice were tested three times 30 minutes after drug administration. The end point of the experiment was defined as the time at which the mice fell from the apparatus or rolled over the rod by holding onto it. The latency to the end point was recorded and analyzed.

Results

ML382 inhibits persistent pain in an MrgprX1-dependent manner

ML382 was applied intrathecally (25 μM, 10 μL) half an hour before formalin (2% formaldehyde, 10 μL) was injected into the plantar aspect of one hind paw. The acute pain

response (first 10 minutes post-formalin) was not affected, but the inflammatory pain response (10 to 60 minutes post-formalin) was significantly attenuated by ML382 in humanized MrgprX1 mice but not in *Mrgpr-clusterΔ*$^{-/-}$ mice (Fig. 4.1A,B).

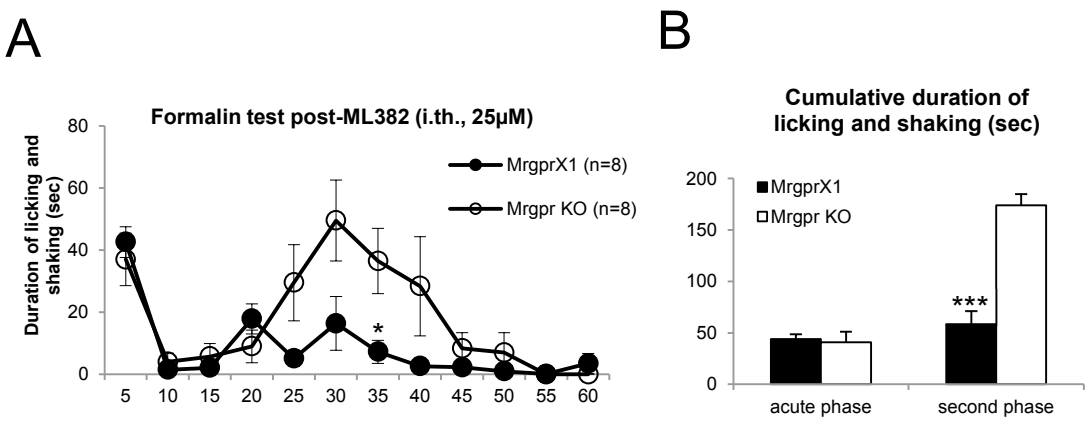

Figure 4.1 ML382 attenuates formalin induced second phase pain without exogenous BAM8–22. (A) ML382 significantly reduced formalin-induced pain during the second phase. **P* < 0.05. **(B)** Cumulative duration of paw licking and shaking after formalin injection showed that the second phase of pain behavior was significantly reduced in MrgprX1 animals. ****P* < 0.0001 vs Mrgpr KO mice. Paired Student's *t*-test was used for statistical analysis.

We then induced inflammation by intraplantar injection of CFA and quantified heat sensitivity with the Hargreaves test. We measured response before and 1 day after CFA injection to confirm the development of inflammation. Then, mice were anesthetized with isoflurane and injected intrathecally with ML382 (25, 125, or 250 µM in 10 µL). A half hour after recovery from isoflurane, response was measured again. We found that ML382 significantly attenuated heat sensitivity in humanized MrgprX1 mice but not in *Mrgpr-clusterΔ*$^{-/-}$ mice (Fig. 4.2A,B). Contralateral heat sensation was not altered by CFA or ML382 administration (Fig. 4.2C,D).

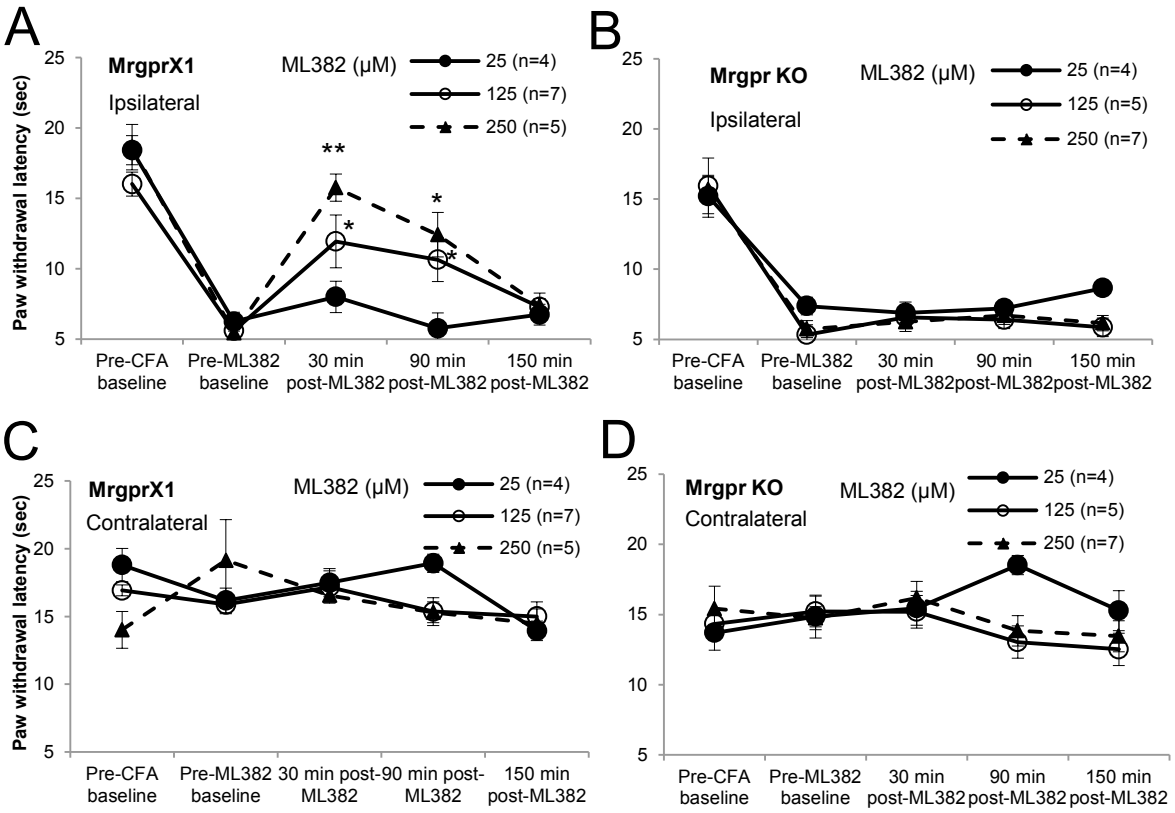

Figure 4.2 CFA induced persistent inflammatory pain was attenuated by ML382. (A) Complete Freund's adjuvant (CFA)-induced heat hypersensitivity of the ipsilateral hind paw was dose-dependently attenuated by ML382. Paw withdrawal latency measured with the Hargreaves test. **P* < 0.05, ***P* <0.01 vs pre-ML382 baseline. **(B)** ML382 was not effective in Mrgpr KO mice. Contralateral heat sensation was not altered by CFA injection or ML382 in either MrgprX1 **(C)** or Mrgpr KO mice **(D)**. Paired Student's *t*-test was used for statistical analysis.

We also performed CCI to induce neuropathic pain and quantified heat sensitivity with the Hargreaves test. We measured response before and 2 weeks after surgery to confirm the development of neuropathic pain. Again we found that ML382 significantly attenuated heat sensitivity in humanized MrgprX1 mice but not in *Mrgpr-clusterΔ*$^{-/-}$ mice (Fig. 4.3A,B). Contralateral heat sensation was not altered by CCI or ML382 administration (Fig. 4.3C,D).

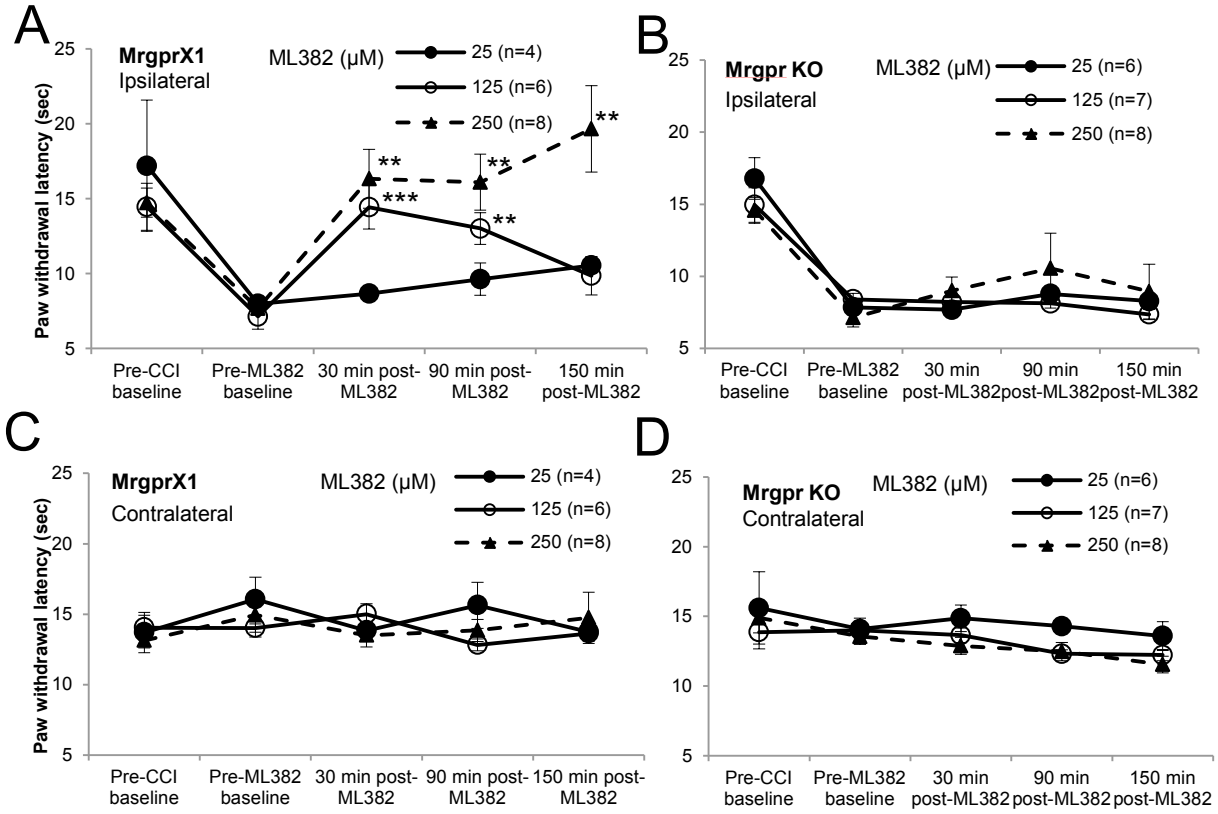

Figure 4.3 CCI induced persistent neuropathic pain was attenuated by ML382. (A) Chronic constriction injury (CCI)-induced heat hypersensitivity of the ipsilateral hind paw was dose-dependently attenuated by ML382. ***P* < 0.01, ****P* < 0.001 vs pre-ML382 baseline. **(B)** ML382 was not effective in Mrgpr KO mice. Contralateral heat sensation was not altered by CCI or ML382 in either MrgprX1 **(C)** or Mrgpr KO mice **(D)**. Paired Student's *t*-test was used for statistical analysis.

ML382 induces conditioned place preference selectively in nerve-injured humanized MrgprX1 mice

Clinically, spontaneous pain is a debilitating aspect of neuropathic pain caused by neuropathic spontaneous discharge in somatosensory neurons (Bennett, 2012). It can be studied in rodents with a conditioned preference paradigm, which can unveil the rewarding effect of pain relief (King et al., 2009). In humanized MrgprX1 mice that had undergone CCI, lumbar puncture injection of ML382 (250 μM, 10-12 μL) led to a significant increase in post-conditioning time spent in an ML382-paired chamber, as compared to the pre-conditioning value (Fig. 4.4A). Simultaneously, the mice decreased time spent in the vehicle (saline)-paired chamber (Fig. 4.4A). However, *Mrgpr-clusterΔ*$^{-/-}$ mice showed no significant change in post-conditioning time spent in the ML382- or vehicle-paired chamber, as compared to the respective pre-conditioning values (Fig. 4.4A). The difference score (Post-conditioning time – Pre-conditioning time) confirmed that only MrgprX1 mice showed a preference for the ML382-paired chamber (Fig. 4.4B). *Mrgpr-clusterΔ*$^{-/-}$ mice showed neither preference nor aversion to ML382 treatment (Fig. 4.4A,B). These results suggest that allosteric modulator ML382 is sufficient to alleviate ongoing pain in humanized MrgprX1 mice with endogenous BAM peptides as orthosteric ligand. The amount of endogenous BAM peptide in the dorsal spinal cord involved is sufficiently (as is supported by HPLC data in Fig. 3.7). Importantly, ML382 did not induce conditioned place preference in naïve animals, suggesting that induction occurs solely by relief from ongoing pain and that the drug itself is not rewarding (Fig. 4.4C,D). Clonidine was used in CCI neuropathic pain animal model as positive control compound for CPP, and clonidine in naïve animals as negative control for CPP. The results showed that clonidine successfully induced CPP in injured animals regardless of genotypes (Fig. 4.5A,B) but not in naïve animals (Fig. 4.5C,D).

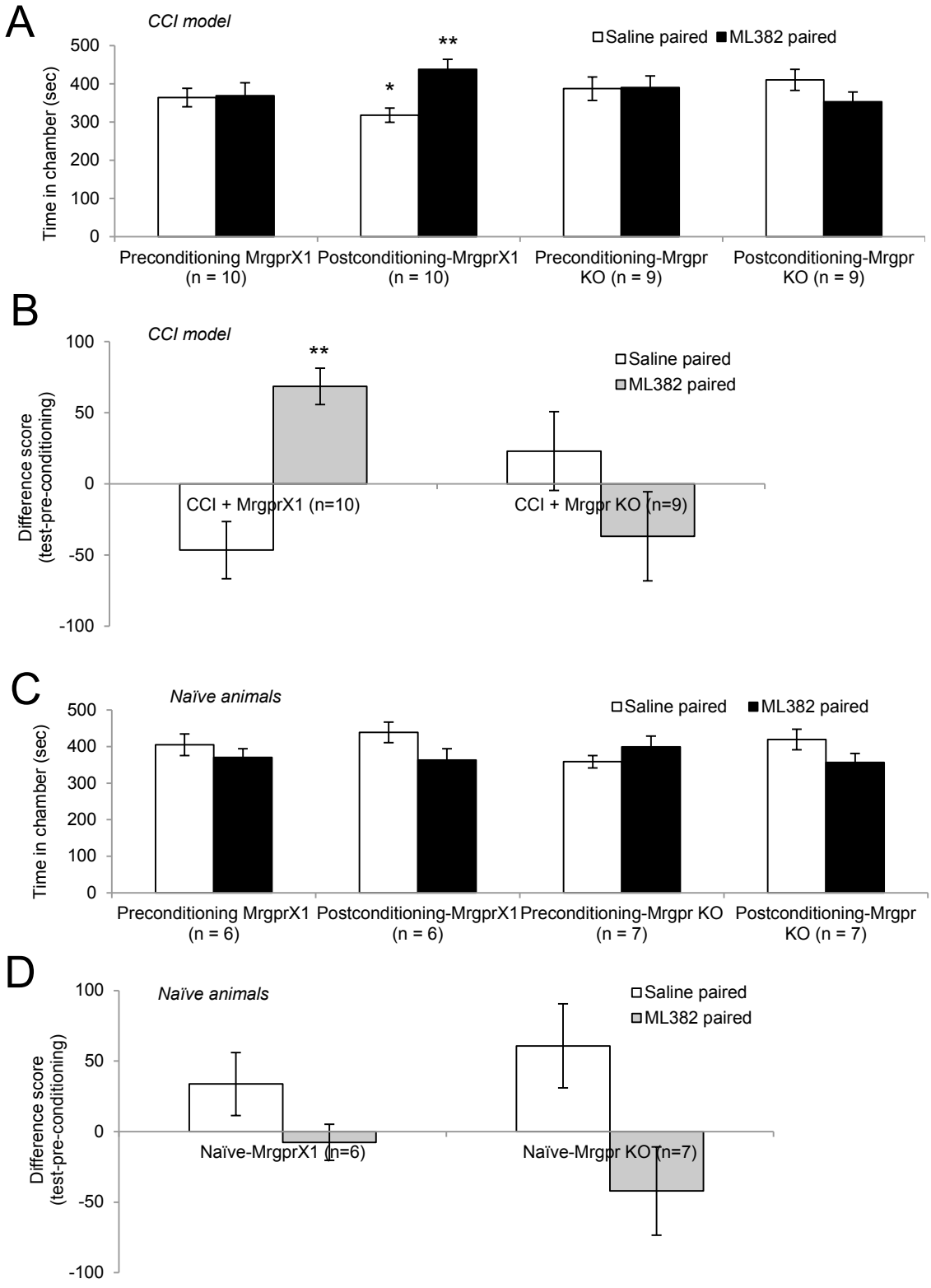
A
CCI model
Saline paired
ML382 paired
Time in chamber (sec)
500
400
300
200
100
0
*
**
Preconditioning MrgprX1 (n = 10)
Postconditioning-MrgprX1 (n = 10)
Preconditioning-Mrgpr KO (n = 9)
Postconditioning-Mrgpr KO (n = 9)
B
CCI model
Saline paired
ML382 paired
Difference score (test-pre-conditioning)
100
50
0
-50
-100
**
CCI + MrgprX1 (n=10)
CCI + Mrgpr KO (n=9)
C
Naïve animals
Saline paired
ML382 paired
Time in chamber (sec)
500
400
300
200
100
0
Preconditioning MrgprX1 (n = 6)
Postconditioning-MrgprX1 (n = 6)
Preconditioning-Mrgpr KO (n = 7)
Postconditioning-Mrgpr KO (n = 7)
D
Naïve animals
Saline paired
ML382 paired
Difference score (test-pre-conditioning)
100
50
0
-50
-100
Naïve-MrgprX1 (n=6)
Naïve-Mrgpr KO (n=7)

Figure 4.4 ML382 induces conditioned place preference in MrgprX1 animals without exogenous BAM8–22. (A) MrgprX1 and Mrgpr KO mice were subjected to chronic constriction injury (CCI) of the sciatic nerve. MrgprX1 mice spent significantly more time in the ML382-paired chamber and less time in the saline-paired chamber compared to times at pre-conditioning baseline. Mrgpr KO mice did not develop preference for or aversion to the ML382-paired chamber. *$P < 0.05$, **$P < 0.01$ vs pre-conditioning baseline. **(B)** The difference score confirmed that only MrgprX1 mice showed preference for the ML382-paired chamber. **$P < 0.01$ vs saline-paired chamber. Statistical power is 0.978 in MrgprX1 animals. **(C)** In the uninjured, naïve condition, neither MrgprX1 nor Mrgpr KO mice developed preference for or aversion to the ML382-paired chamber. **(D)** This finding was confirmed by the difference score. Two-factor repeated ANOVA, Bonferroni *post hoc* test was used for statistical analysis.

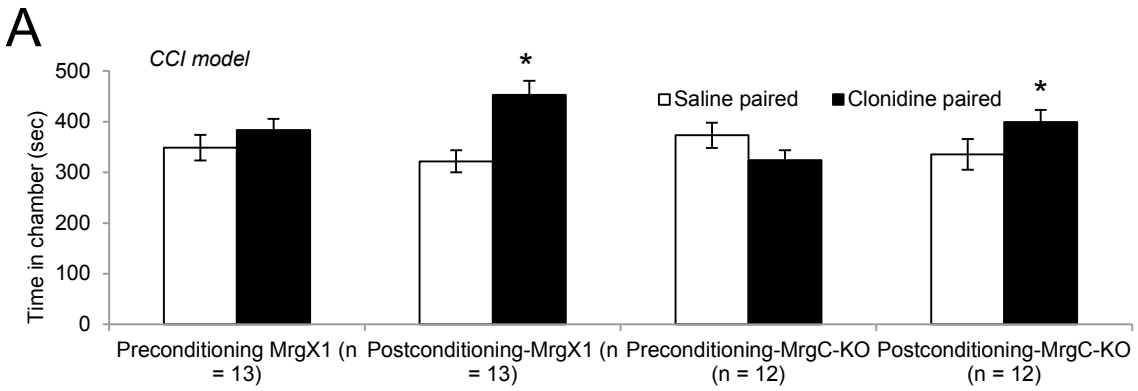
A
CCI model
Saline paired
Clonidine paired
Time in chamber (sec)
500
400
300
200
100
0
*
*
Preconditioning MrgX1 (n = 13)
Postconditioning-MrgX1 (n = 13)
Preconditioning-MrgC-KO (n = 12)
Postconditioning-MrgC-KO (n = 12)

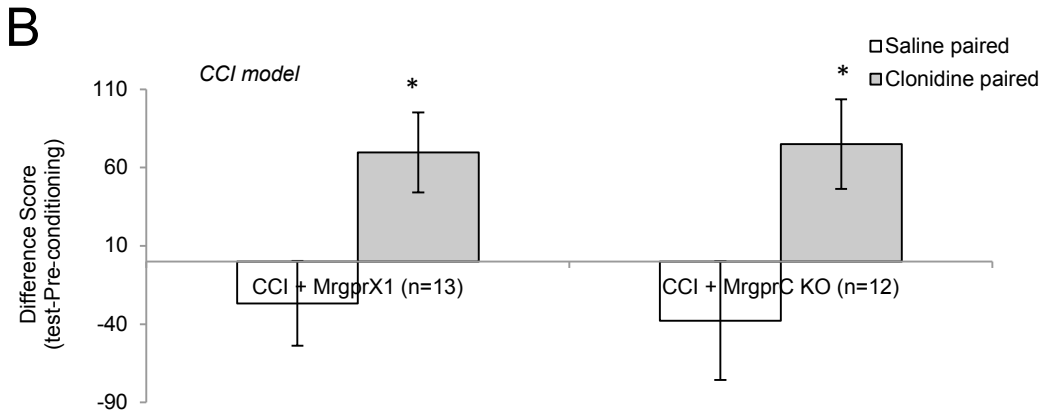
B
CCI model
Saline paired
Clonidine paired
Difference Score (test-Pre-conditioning)
110
60
10
-40
-90
*
*
CCI + MrgprX1 (n=13)
CCI + MrgprC KO (n=12)

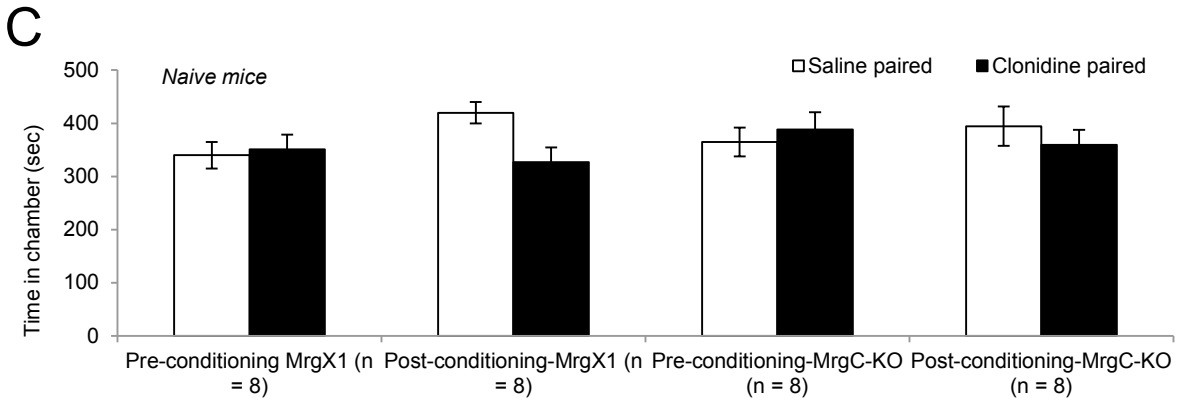
C
Naive mice
Saline paired
Clonidine paired
Time in chamber (sec)
500
400
300
200
100
0
Pre-conditioning MrgX1 (n = 8)
Post-conditioning-MrgX1 (n = 8)
Pre-conditioning-MrgC-KO (n = 8)
Post-conditioning-MrgC-KO (n = 8)

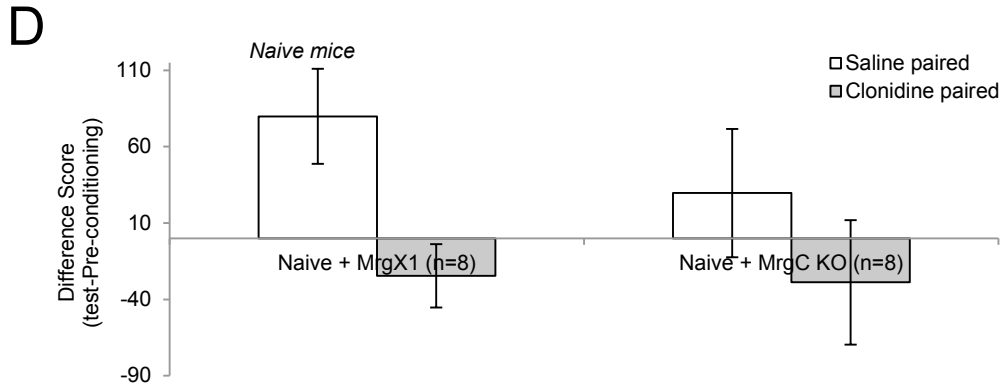
D
Naive mice
Saline paired
Clonidine paired
Difference Score (test-Pre-conditioning)
110
60
10
-40
-90
Naive + MrgX1 (n=8)
Naive + MrgC KO (n=8)

Figure 4.5 Positive control of conditioned place reference induced by clonidine. **(A)** Intrathecally delivered clonidine (1 μg dissolved in 5 μL saline) induced chamber preference in CCI mice, regardless of genotypes. * $P < 0.05$ vs preconditioning baseline. **(B)** The difference score confirmed that both genotypes showed preference for the clonidine-paired chamber. *P < 0.05 vs saline-paired chamber. Statistical power is 0.700 in MrgprX1 animals and 0.620 in Mrgpr KO animals. **(C)** Same dose of clonidine did not induce chamber preference in naïve mice, regardless of genotypes. **(D)** The difference score confirmed that neither genotypes showed preference for the clonidine-paired chamber. Two-factor repeated ANOVA, Bonferroni *post hoc* test was used for statistical analysis.

ML382 does not induce scratching behavior or impair motor function

Besides inhibiting pain, Mrgprs also function as itch receptors in the peripheral terminals. BAM8–22 inhibits pain but also induces scratching behavior when injected subcutaneously (Fig. 4.6A) (Liu et al., 2009; Sikand et al., 2011; Han et al., 2013). We scored mice for scratching behavior after ML382 was applied subcutaneously into the back, intraperitoneally, or intrathecally. We did not observe a significant difference between the humanized MrgprX1 group and *Mrgpr-clusterΔ*$^{-/-}$ group, indicating that ML382 does not induce itch (Fig. 4.6A). Moreover, ML382 (250 μM, 10-12 μL, i.th.) did not affect locomotor function in naïve animals of either genotype (Fig. 4.6B).

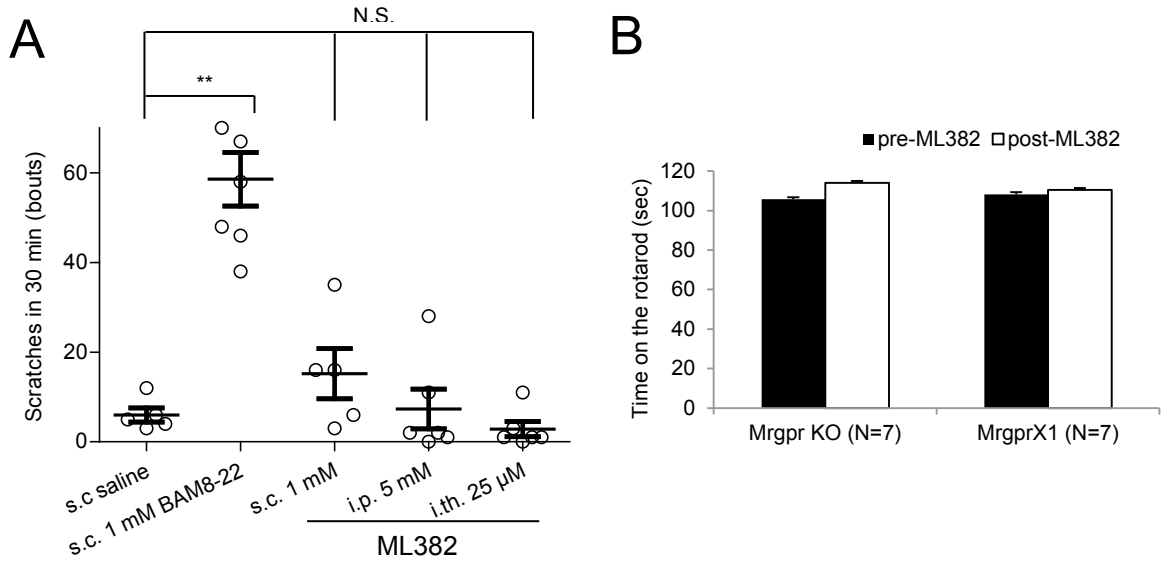

Figure 4.6 ML382 did not induce scratching behavior or impair motor function. (A) ML382 did not induce scratching behavior when applied subcutaneously (s.c.) into the back, intraperitoneally (i.p.), or intrathecally (i.th.) in humanized MrgprX1 mice. Subcutaneous injection of BAM8–22 caused rigorous scratching behavior. *n* = 5-7 for each treatment. N.S. stands for not statistically significant. **(B)** Naïve (uninjured) humanized MrgprX1 mice and *Mrgpr-clusterΔ*$^{-/-}$ mice did not differ in motor function as measured by rotarod test. Neither group was affected after an intrathecal injection of 250 μM ML382.

Discussion

Our study also revealed that ML382 produced conditioned place preference to the relief of CCI-induced ongoing neuropathic pain. Operant behavior studies such as the conditioned place test measure the affective/aversive aspect of spontaneous pain experience, which relates closely to the complex human experience of chronic pain (Navratilova et al., 2013). One example involves spinal administration of adenosine, which blocked evoked hyperalgesia in patients with neuropathic pain but failed to alleviate overall ongoing pain (Eisenach et al., 2003). Intrathecal administration of adenosine in the rat model of spinal nerve ligation-induced neuropathic pain revealed that adenosine reversed tactile hypersensitivity but failed to produce conditioned place preference (King et al., 2009). Therefore, this operant behavior study is of high translational relevance and indicates that ML382 is a promising anti-pain compound. Furthermore, ML382 was not rewarding in naïve animals. This feature is important because it suggests a low likelihood for abuse.

One limitation of ML382 is that it is not effective in inhibiting mechanical allodynia induced by CFA injection in the hind paw or sciatic nerve CCI as detected by von Frey fiber (data not shown). A possible explanation is that ML382 is allosteric modulator that can maximize but not surpass the effect of the orthosteric agonist BAM8–22. According to Jiang et al. (Jiang et al., 2013), BAM8–22 (i.th. 30nmol) did not change CFA-induced mechanical hypersensitivity of male Sprague-Dawley rats. Therefore ML382 might also be limited in its ability to inhibit mechanical allodynia through Mrgpr pathway. However, BAM8–22 (i.th. 1 mM, 5 μL) was reported to attenuate mechanical allodynia (assessed by von Frey fiber) as well as thermal hyperalgesia (assessed by Hargreaves test) of persistent inflammatory (induced by intraplantar CFA injection) and neuropathic pain (induced by sciatic nerve CCI) in wild type C57BL/6 mice (Guan et al., 2010). MrgprC selective agonist JHU58 (i.th. 0.5 mM, 5 μL), a peptidomimetic of Arg-Phe-NH_2, was also reported to inhibit attenuate both mechanical allodynia and thermal hyperalgesia in MrgprC dependent manner (He et al., 2014). Therefore, mouse MrgprC11, rat MrgprC and

human MrgprX1 might differ in their downstream effect of fine tuning thermal hyperalgesia or mechanical allodynia. It is notable that BAM8–22 and JHU58 at their antinociceptive dose induce mild irritation (e.g., scratching and tail-flicking) in wild type and KO animals (Guan et al., 2010; He et al., 2014), which was not observed in the case of ML382. This suggested that MrgprC agonists possess nonselective action in an MrgprC independent manner or they function through Mrgpr family members that are not one of the twelve deleted Mrgpr cluster (He et al., 2014). Allosteric modulation requires the presence of both the receptor and orthosteric agonist, therefore can avoid potential nonselective/off-target action where another closely related Mrgpr member is present but its endogenous orthosteric agonist is not or vice versa.

CHAPTER 5: CONCLUSION AND FUTURE DIRECTIONS

A major goal of this thesis is to develop a pain-selective pharmacological intervention that targets at nociceptive sensory neurons at periphery. Accordingly, we screened small molecular compounds targeting at human MrgprX1 receptor. *Mrgprs* are a family of orphan G-protein-coupled receptors (GPCRs) consisting of many genes in human, rat, and mouse (Dong et al., 2001; Lembo et al., 2002; Choi and Lahn, 2003; Zhang et al., 2005; Gloriam et al., 2007). Previous work has implicated that many *Mrgpr*s, including human *MrgprX1*, are expressed specifically in small-diameter afferent neurons (presumably nociceptive) and have been reported to play important roles in somatosensation of pain and itch (Zylka et al., 2003; Conn et al., 2009; Liu et al., 2009; Guan et al., 2010; Sikand et al., 2011; Liu et al., 2012; Han et al., 2013; He et al., 2014; He et al., 2014). Using calcium mobilization functional assays in HEK293 heterologous system stably express MrgprX1, we found that some drug candidates act on MrgprX1 as allosteric modulators at the presence of BAM8–22 as the orthosteric agonist. Allosteric modulators often can offer proper temporal and spatial control of endogenous physiological signaling because of the requirement for the presence of endogenous orthosteric ligand. To confirm the *in vivo* function, we established a transgenic mouse line in which human *MrgprX1* gene is expressed in *Mrgpr*-expressing primary sensory DRG neurons. This valuable humanized mouse line allowed us to do animals tests because the mouse Mrgprs are not responsive to many MrgprX1 agonists or modulators including ML382. Using electrophysiology study on neuronal culture, we found that ML382 enhanced the ability of MrgprX1 to inhibit N-type channels and block presynaptic terminal function. Immunostaining results and HPLC analysis also implicated an increase amount of endogenous BAM peptide at injury condition. Based on the above findings we next performed behavioral study and evaluated the analgesic effect of ML382. We showed that ML382 also effectively attenuated evoked persistent pain and spontaneous pain *in vivo*, without causing central or peripheral side effects such as itch.

ML382 is a promising anti-pain compound since it can inhibit neuropathic pain in both sensory dimension and affective dimension, and may have good effectiveness in patients with ongoing spontaneous neuropathic pain. Furthermore, ML382 induced CPP was not observed in naïve animals, suggesting it relieved ongoing pain instead of being rewarding itself. Interestingly, we were only able to observe analgesic effect when ML382 is given i.th. but not i.p. or subcutaneously (data not shown). Further modification of the structure of ML382 is in progress, aiming to improve the penetration ability across blood brain barrier to reach central terminals of primary sensory neurons in the spinal cord so that it could be administrated systemically instead of intrathecally.

REFERENCES

Bao, J., J. J. Li, et al. (1998). "Differences in Ca2+ channels governing generation of miniature and evoked excitatory synaptic currents in spinal laminae I and II." J Neurosci **18**(21): 8740-8750.

Basbaum, A. I., D. M. Bautista, et al. (2009). "Cellular and molecular mechanisms of pain." Cell **139**(2): 267-284.

Basbaum, A. I. and T. Jessell (2000). The perception of pain. Principles of Neuroscience. E. R. Kandel, J. Schwartz and T. Jessell. New York, Appleton and Lange**:** 472-491.

Bennett, G. J. (2012). "What is spontaneous pain and who has it?" J Pain **13**(10): 921-929.

Bourinet, E., T. W. Soong, et al. (1996). "Determinants of the G protein-dependent opioid modulation of neuronal calcium channels." Proc Natl Acad Sci U S A **93**(4): 1486-1491.

Breivik, H., B. Collett, et al. (2006). "Survey of chronic pain in Europe: prevalence, impact on daily life, and treatment." Eur J Pain **10**(4): 287-333.

Cai, M., T. Chen, et al. (2007). "The involvement of spinal bovine adrenal medulla 22-like peptide, the proenkephalin derivative, in modulation of nociceptive processing." Eur J Neurosci **26**(5): 1128-1138.

Catterall, W. A. (2000). "Structure and regulation of voltage-gated Ca2+ channels." Annu Rev Cell Dev Biol **16**: 521-555.

Chen, H. and S. R. Ikeda (2004). "Modulation of ion channels and synaptic transmission by a human sensory neuron-specific G-protein-coupled receptor, SNSR4/mrgX1, heterologously expressed in cultured rat neurons." J Neurosci **24**(21): 5044-5053.

Chen, P., Y. Liu, et al. (2008). "Effect of chronic administration of morphine on the expression of bovine adrenal medulla 22-like immunoreactivity in the spinal cord of rats." Eur J Pharmacol **589**(1-3): 110-113.

Choi, S. S. and B. T. Lahn (2003). "Adaptive evolution of MRG, a neuron-specific gene family implicated in nociception." Genome Res **13**(10): 2252-2259.

Conn, P. J., A. Christopoulos, et al. (2009). "Allosteric modulators of GPCRs: a novel approach for the treatment of CNS disorders." Nat Rev Drug Discov **8**(1): 41-54.

Cox, J. J., J. Sheynin, et al. (2010). "Congenital insensitivity to pain: novel SCN9A missense and in-frame deletion mutations." Hum Mutat **31**(9): E1670-1686.

De Lean, A., J. M. Stadel, et al. (1980). "A ternary complex model explains the agonist-specific binding properties of the adenylate cyclase-coupled beta-adrenergic receptor." J Biol Chem **255**(15): 7108-7117.

Dong, X., S. Han, et al. (2001). "A diverse family of GPCRs expressed in specific subsets of nociceptive sensory neurons." Cell **106**(5): 619-632.

Ehlert, F. J. (1988). "Estimation of the Affinities of Allosteric Ligands Using Radioligand Binding and Pharmacological Null Methods." Molecular Pharmacology **33**(2): 187-194.

Eisenach, J. C., R. L. Rauck, et al. (2003). "Intrathecal, but not intravenous adenosine reduces allodynia in patients with neuropathic pain." Pain **105**(1-2): 65-70.

Fields, H. L. (1999). "Pain: an unpleasant topic." Pain **Suppl 6**: S61-69.

Fields, H. L. (2007). "Understanding how opioids contribute to reward and analgesia." Reg Anesth Pain Med **32**(3): 242-246.

Fox, A. P., M. C. Nowycky, et al. (1987). "Kinetic and pharmacological properties distinguishing three types of calcium currents in chick sensory neurones." J Physiol **394**: 149-172.

George, S. R., B. F. O'Dowd, et al. (2002). "G-protein-coupled receptor oligomerization and its potential for drug discovery." Nat Rev Drug Discov **1**(10): 808-820.

Gloriam, D. E., R. Fredriksson, et al. (2007). "The G protein-coupled receptor subset of the rat genome." BMC Genomics **8**: 338.

Gribkoff, V. K. (2006). "The role of voltage-gated calcium channels in pain and nociception." Semin Cell Dev Biol **17**(5): 555-564.

Guan, Y., Q. Liu, et al. (2010). "Mas-related G-protein-coupled receptors inhibit pathological pain in mice." Proc Natl Acad Sci U S A **107**(36): 15933-15938.

Guan, Y., F. Yuan, et al. (2010). "A partial L5 spinal nerve ligation induces a limited prolongation of mechanical allodynia in rats: an efficient model for studying mechanisms of neuropathic pain." Neurosci Lett **471**(1): 43-47.

Han, L., C. Ma, et al. (2013). "A subpopulation of nociceptors specifically linked to itch." Nat Neurosci **16**(2): 174-182.

Han, S. K., X. Dong, et al. (2002). "Orphan G protein-coupled receptors MrgA1 and MrgC11 are distinctively activated by RF-amide-related peptides through the Galpha q/11 pathway." Proc Natl Acad Sci U S A **99**(23): 14740-14745.

He, S. Q., L. Han, et al. (2014). "Temporal changes in MrgC expression after spinal nerve injury." Neuroscience **261**: 43-51.

He, S. Q., Z. Li, et al. (2014). "MrgC agonism at central terminals of primary sensory neurons inhibits neuropathic pain." Pain **155**(3): 534-544.

Heinl, C., R. Drdla-Schutting, et al. (2011). "Distinct mechanisms underlying pronociceptive effects of opioids." J Neurosci **31**(46): 16748-16756.

Herlitze, S., D. E. Garcia, et al. (1996). "Modulation of Ca2+ channels by G-protein beta gamma subunits." Nature **380**(6571): 258-262.

Hescheler, J., W. Rosenthal, et al. (1987). "The GTP-binding protein, Go, regulates neuronal calcium channels." Nature **325**(6103): 445-447.

Hille, B., D. J. Beech, et al. (1995). "Multiple G-protein-coupled pathways inhibit N-type Ca channels of neurons." Life Sci **56**(11-12): 989-992.

Hollt, V., I. Haarmann, et al. (1982). "Pro-enkephalin intermediates in bovine brain and adrenal medulla: characterization of immunoreactive peptides related to BAM-22P and peptide F." Life Sci **31**(16-17): 1883-1886.

Ji, R. R., T. Kohno, et al. (2003). "Central sensitization and LTP: do pain and memory share similar mechanisms?" Trends Neurosci **26**(12): 696-705.

Jiang, J., D. Wang, et al. (2013). "Effect of Mas-related gene (Mrg) receptors on hyperalgesia in rats with CFA-induced inflammation via direct and indirect mechanisms." Br J Pharmacol **170**(5): 1027-1040.

Kamohara, M., A. Matsuo, et al. (2005). "Identification of MrgX2 as a human G-protein-coupled receptor for proadrenomedullin N-terminal peptides." Biochem Biophys Res Commun **330**(4): 1146-1152.

Kaneko, S., K. Fukuda, et al. (1994). "Ca2+ channel inhibition by kappa opioid receptors expressed in Xenopus oocytes." Neuroreport **5**(18): 2506-2508.

King, T., L. Vera-Portocarrero, et al. (2009). "Unmasking the tonic-aversive state in neuropathic pain." Nat Neurosci **12**(11): 1364-1366.

Klotz, U. (2006). "Ziconotide--a novel neuron-specific calcium channel blocker for the intrathecal treatment of severe chronic pain--a short review." Int J Clin Pharmacol Ther **44**(10): 478-483.

Lembo, P. M., E. Grazzini, et al. (2002). "Proenkephalin A gene products activate a new family of sensory neuron--specific GPCRs." Nat Neurosci **5**(3): 201-209.

Li, Z., S. Q. He, et al. (2014). "Activation of MrgC receptor inhibits N-type calcium channels in small-diameter primary sensory neurons in mice." Pain **155**: 1613-1621.

Liu, Q., P. Sikand, et al. (2012). "Mechanisms of itch evoked by beta-alanine." J Neurosci **32**(42): 14532-14537.

Liu, Q., Z. Tang, et al. (2009). "Sensory neuron-specific GPCR Mrgprs are itch receptors mediating chloroquine-induced pruritus." Cell **139**(7): 1353-1365.

Macdonald, R. L. and M. A. Werz (1986). "Dynorphin A decreases voltage-dependent calcium conductance of mouse dorsal root ganglion neurones." J Physiol **377**: 237-249.

May, L. T., K. Leach, et al. (2007). "Allosteric modulation of G protein-coupled receptors." Annu Rev Pharmacol Toxicol **47**: 1-51.

McGivern, J. G. and S. I. McDonough (2004). "Voltage-gated calcium channels as targets for the treatment of chronic pain." Curr Drug Targets CNS Neurol Disord **3**(6): 457-478.

Mizuno, K., N. Minamino, et al. (1980). "A new family of endogenous "big" Met-enkephalins from bovine adrenal medulla: purification and structure of docosa- (BAM-22P) and eicosapeptide (BAM-20P) with very potent opiate activity." Biochem Biophys Res Commun **97**(4): 1283-1290.

Mohler, H., J. M. Fritschy, et al. (2002). "A new benzodiazepine pharmacology." J Pharmacol Exp Ther **300**(1): 2-8.

Moises, H. C., K. I. Rusin, et al. (1994). "mu-Opioid receptor-mediated reduction of neuronal calcium current occurs via a G(o)-type GTP-binding protein." J Neurosci **14**(6): 3842-3851.

Navratilova, E., J. Y. Xie, et al. (2013). "Evaluation of reward from pain relief." Ann N Y Acad Sci **1282**: 1-11.

Perret, D. and Z. D. Luo (2009). "Targeting voltage-gated calcium channels for neuropathic pain management." Neurotherapeutics **6**(4): 679-692.

Pope, J. E., T. R. Deer, et al. (2013). "A systematic review: current and future directions of dorsal root ganglion therapeutics to treat chronic pain." Pain Med **14**(10): 1477-1496.

Portenoy, R. K. (1996). "Opioid therapy for chronic nonmalignant pain: a review of the critical issues." J Pain Symptom Manage **11**(4): 203-217.

Qin, N., D. Platano, et al. (1997). "Direct interaction of gbetagamma with a C-terminal gbetagamma-binding domain of the Ca2+ channel alpha1 subunit is responsible for channel inhibition by G protein-coupled receptors." Proc Natl Acad Sci U S A **94**(16): 8866-8871.

Raingo, J., A. J. Castiglioni, et al. (2007). "Alternative splicing controls G protein-dependent inhibition of N-type calcium channels in nociceptors." Nat Neurosci **10**(3): 285-292.

Samama, P., S. Cotecchia, et al. (1993). "A mutation-induced activated state of the beta 2-adrenergic receptor. Extending the ternary complex model." J Biol Chem **268**(7): 4625-4636.

Scholz, J. and C. J. Woolf (2002). "Can we conquer pain?" Nat Neurosci **5 Suppl**: 1062-1067.

Sikand, P., X. Dong, et al. (2011). "BAM8-22 peptide produces itch and nociceptive sensations in humans independent of histamine release." J Neurosci **31**(20): 7563-7567.

Solinski, H. J., T. Gudermann, et al. (2014). "Pharmacology and signaling of MAS-related G protein-coupled receptors." Pharmacol Rev **66**(3): 570-597.

Staats, P. S., T. Yearwood, et al. (2004). "Intrathecal ziconotide in the treatment of refractory pain in patients with cancer or AIDS: a randomized controlled trial." JAMA **291**(1): 63-70.

Tedford, H. W. and G. W. Zamponi (2006). "Direct G protein modulation of Cav2 calcium channels." Pharmacol Rev **58**(4): 837-862.

Tsunoo, A., M. Yoshii, et al. (1986). "Block of calcium channels by enkephalin and somatostatin in neuroblastoma-glioma hybrid NG108-15 cells." Proc Natl Acad Sci U S A **83**(24): 9832-9836.

Wen, W., Y. Wang, et al. (2015). "Discovery and Characterization of 2-(Cyclopropanesulfonamido)-N-(2-ethoxyphenyl)benzamide, ML382: a Potent and Selective Positive Allosteric Modulator of MrgX1." ChemMedChem **10**(1): 57-61.

Wermeling, D. P. (2005). "Ziconotide, an intrathecally administered N-type calcium channel antagonist for the treatment of chronic pain." Pharmacotherapy **25**(8): 1084-1094.

Wiley, J. W., H. C. Moises, et al. (1997). "Dynorphin A-mediated reduction in multiple calcium currents involves a G(o) alpha-subtype G protein in rat primary afferent neurons." J Neurophysiol **77**(3): 1338-1348.

Wilson, S. R., K. A. Gerhold, et al. (2011). "TRPA1 is required for histamine-independent, Mas-related G protein-coupled receptor-mediated itch." Nature Neuroscience **14**(5): 595-602.

Woolf, C. J. and M. W. Salter (2000). "Neuronal plasticity: increasing the gain in pain." Science **288**(5472): 1765-1769.

Yusaf, S. P., J. Goodman, et al. (2001). "Expression of voltage-gated calcium channel subunits in rat dorsal root ganglion neurons." Neurosci Lett **311**(2): 137-141.

Zamponi, G. W. and K. P. Currie (2013). "Regulation of Ca(V)2 calcium channels by G protein coupled receptors." Biochim Biophys Acta **1828**(7): 1629-1643.

Zhang, L., N. Taylor, et al. (2005). "Cloning and expression of MRG receptors in macaque, mouse, and human." Brain Res Mol Brain Res **133**(2): 187-197.

Zylka, M. J., X. Dong, et al. (2003). "Atypical expansion in mice of the sensory neuron-specific Mrg G protein-coupled receptor family." Proc Natl Acad Sci U S A **100**(17): 10043-10048.

CURRICULUM VITAE FOR Ph.D. CANDIDATES

The Johns Hopkins University School of Medicine

ZHE LI Jan. 20, 2015

The Solomon H. Snyder Department of Neuroscience

725 N. Wolfe Street, WBSB 908, Baltimore, MD 21205

Lab phone: (410) 502-2968 E-mail: zli38@jhmi.edu

Educational History

Ph.D. expected 2016		Program in BCMB Mentor: Xinzhong Dong, Ph.D.	Johns Hopkins University School of Medicine
B.S.	2010	Biological Sciences	Zhejiang University

Other Professional Experience

Research Rotation of Medicine	2011	Lab of Alex L. Kolodkin, Ph.D.	Johns Hopkins University School
Research Rotation of Medicine	2010	Lab of Jie Xiao, Ph.D.	Johns Hopkins University School
Research volunteer	2009	Lab of Ted Powers, Ph.D.	University of California, Davis
Summer Research School	2008	Lab of Kristen J. Verhey, Ph.D	University of Michigan Medical
Research assistant	2007	Lab of Wanxi Yang, Ph.D	Zhejiang University

Peer Reviewed Publications

Li Z, He SQ, Tseng PY, Xu Q, Tiwari V, Yang F, Shu B, Zhang T, Tang Z, Raja SN, Wang Y, Dong X, Guan Y. (2015) The inhibition of high-voltage-activated calcium current by activation of MrgC11 involves phospholipase C-dependent mechanisms. *Neuroscience*. 300: 393-403. PMCID: PMC4485588

Wen W, Wang Y, **Li Z**, Tseng PY, McManus OB, Wu M, Li M, Lindsley CW, Dong X, Hopkins CR. (2015) Discovery and characterization of 2-(cyclopropanesulfonamido)-N-(2-ethoxyphenyl)benzamide, ML382: a potent and selective positive allosteric modulator of MrgX1. *ChemMedChem.* 10:57-61. PMCID: PMC4276534

Kim YJ, Lim H, **Li Z**, Oh Y, Kovlyagina I, Choi IY, Dong X, Lee G. (2014) Generation of multipotent induced neural crest by direct reprogramming of human postnatal fibroblasts with a single transcription factor. *Cell Stem Cell*. 15:497-506. PMID: 25158936 (no PMCID available)

Li Z, He SQ, Xu Q, Yang F, Tiwari V, Liu Q, Tang Z, Han L, Chu YX, Wang Y, Hin N, Tsukamoto T, Slusher B, Guan X, Wei F, Raja SN, Dong X, Guan Y. (2014) Activation of MrgC receptor

inhibits N-type calcium channels in small-diameter primary sensory neurons in mice. *Pain*. 155:1613-21. PMCID: PMC4104261

Kim YS, Chu Y, Han L, Li M, **Li Z**, Lavinka PC, Sun S, Tang Z, Park K, Caterina MJ, Ren K, Dubner R, Wei F, Dong X. (2014) Central terminal sensitization of TRPV1 by descending serotonergic facilitation modulates chronic pain. *Neuron*. 81:873-87. PMCID: PMC3943838

He SQ*, **Li Z***, Chu YX, Han L, Xu Q, Li M, Yang F, Liu Q, Tang Z, Wang Y, Hin N, Tsukamoto T, Slusher B, Tiwari V, Shechter R, Wei F, Raja SN, Dong X, Guan Y. (2014) MrgC agonism at central terminals of primary sensory neurons inhibits neuropathic pain. *Pain*. 155:534-44. PMCID: PMC3945061 *Co-first authorship

He SQ, Han L, **Li Z**, Xu Q, Tiwari V, Yang F, Guan X, Wang Y, Raja SN, Dong X, Guan Y. (2014) Temporal changes in MrgC expression after spinal nerve injury. Neuroscience. 261:43-51. PMCID: PMC3945476

Han L, Ma C, Liu Q, Weng HJ, Cui Y, Tang Z, Kim Y, Nie H, Qu L, Patel KN, **Li Z**, McNeil B, He S, Guan Y, Xiao B, Lamotte RH, Dong X. (2013) A subpopulation of nociceptors specifically linked to itch. *Nat Neurosci.* 16:174-82. PMCID: PMC3557753

Liu Q, Sikand P, Ma C, Tang Z, Han L, **Li Z**, Sun S, LaMotte RH, Dong X. (2012) Mechanisms of itch evoked by β-alanine. *J Neurosci.* 32:14532-7. PMCID: PMC3491570

Hu JH, Yang L, Kammermeier PJ, Moore CG, Brakeman PR, Tu J, Yu S, Petralia RS, **Li Z**, Zhang PW, Park JM, Dong X, Xiao B, Worley PF. (2012) Preso1 dynamically regulates group I metabotropic glutamate receptors. *Nat Neurosci*. 15:836-44. PMCID: PMC3434267

Li Z, Zhu JQ, Yang WX. (2010) Acrosome reaction in Octopus tankahkeei induced by calcium ionophore A23187 and a possible role of the acrosomal screw. *Micron*. 41:39-46. PMID: 19729317 (no PMCID available)

Hammond JW, Cai D, Blasius TL, **Li Z**, Jiang Y, Jih GT, Meyhofer E, Verhey KJ. (2009) Mammalian Kinesin-3 motors are dimeric in vivo and move by processive motility upon release of autoinhibition. *PLoS Biol*. 31:e72. PMCID: PMC2661964

Poster

Li Z, Tseng PY, Tiwari V, Xu Q, Han L, Sun S, Guan Y, Dong X. (2015) Allosteric modulator of Mas-Related G-Protein Coupled Receptor X1 (MrgprX1) inhibits persistent pain. Howard Hughes Medical Institute Meeting, Ashburn, VA, June 10, 2015.

Community Services

2012 May and 2013 February. Volunteer at Asian American Healthcare Center.

2013 Spring semester. Teaching assistant for Medical Mandarin. Johns Hopkins University School of Medicine.

2014 January to September. Volunteer at post-anesthesia care unit and medical intensive care unit, Great Baltimore Medical Center.

2015 July to October. Volunteer at Baltimore Rescue Mission Clinic.